



This is a repository copy of *Optical, electrochemical, thermal, and structural properties of synthesized fluorene/dibenzosilole-benzothiadiazole dicarboxylic imide alternating organic copolymers for photovoltaic applications*.

White Rose Research Online URL for this paper:
<http://eprints.whiterose.ac.uk/168724/>

Version: Published Version

Article:

R. Murad, A., Iraqi, A. orcid.org/0000-0003-3060-6663, Aziz, S.B. et al. (3 more authors) (2020) Optical, electrochemical, thermal, and structural properties of synthesized fluorene/dibenzosilole-benzothiadiazole dicarboxylic imide alternating organic copolymers for photovoltaic applications. *Coatings*, 10 (12). 1147. ISSN 2079-6412

<https://doi.org/10.3390/coatings10121147>

Reuse

This article is distributed under the terms of the Creative Commons Attribution (CC BY) licence. This licence allows you to distribute, remix, tweak, and build upon the work, even commercially, as long as you credit the authors for the original work. More information and the full terms of the licence here:
<https://creativecommons.org/licenses/>

Takedown




If you consider content in White Rose Research Online to be in breach of UK law, please notify us by emailing eprints@whiterose.ac.uk including the URL of the record and the reason for the withdrawal request.



eprints@whiterose.ac.uk
<https://eprints.whiterose.ac.uk/>

Article

Optical, Electrochemical, Thermal, and Structural Properties of Synthesized Fluorene/Dibenzosilole-Benzothiadiazole Dicarboxylic Imide Alternating Organic Copolymers for Photovoltaic Applications

Ary R. Murad ¹, A. Iraqi ^{2,*} , Shujahadeen B. Aziz ^{3,4,*} , Sozan N. Abdullah ⁵,
Rebar T. Abdulwahid ^{3,6}  and Sarkawt A. Hussien ³

¹ Department of Pharmaceutical Chemistry, College of Medical and Applied Sciences, Charmo University, Chamchamal 46023, Iraq; ary.murad@charmouniversity.org

² Department of Chemistry, University of Sheffield, Sheffield S3 7HF, UK

³ Hameed Majid Advanced Polymeric Materials Research Lab., Department of Physics, College of Science, University of Sulaimani, Qlyasan Street, Sulaimani 46001, Iraq; rebar.abdulwahid@univsul.edu.iq (R.T.A.); sarkawt.hussen@univsul.edu.iq (S.A.H.)

⁴ Department of Civil Engineering, College of Engineering, Komar University of Science and Technology, Sulaimani 46001, Iraq

⁵ Department of Chemistry, College of Science, University of Sulaimani, Qlyasan Street, Sulaimani 46001, Iraq; sozan.abdulla@univsul.edu.iq

⁶ Department of Physics, College of Education, University of Sulaimani, Old Campus, Sulaimani 46001, Iraq

* Correspondence: a.iraqi@sheffield.ac.uk (A.I.); shujahadeenaziz@gmail.com (S.B.A.)

Received: 28 October 2020; Accepted: 16 November 2020; Published: 24 November 2020



Abstract: In this work, four donor–acceptor copolymers, PFDTBTDI-DMO, PFDTBTDI-8, PDBSDTBTDI-DMO, and PDBSDTBTDI-8, based on alternating 2,7-fluorene or 2,7-dibenzosilole flanked by thienyl units, as electron-donor moieties and benzothiadiazole dicarboxylic imide (BTDI) as electron-accepting units, have been designed and synthesized for photovoltaic applications. All polymers were synthesized in good yields via Suzuki polymerization. The impact of attaching two different alkyl chains (3,7-dimethyloctyl vs. *n*-octyl) to the BTDI units upon the solubilities, molecular weights, optical and electrochemical properties, and thermal and structural properties of the resulting polymers was investigated. PFDTBTDI-8 has the highest number average molecular weight ($M_n = 24,900 \text{ g}\cdot\text{mol}^{-1}$) among all polymers prepared. Dibenzosilole-based polymers have slightly lower optical band gaps relative to their fluorene-based analogues. All polymers displayed deep-lying HOMO levels. Their HOMO energy levels are unaffected by the nature of either the alkyl substituents or the donor moieties. Similarly, the LUMO levels are almost identical for all polymers. All polymers exhibit excellent thermal stability with T_d exceeding 350 °C. X-ray powder diffraction (XRD) studies have shown that all polymers have an amorphous nature in the solid state.

Keywords: conductive polymer thin films; fluorene-based polymers; dibenzosilole-based polymers; donor–acceptor copolymers; optical properties; thermal properties; cyclic voltammetry; XRD study

1. Introduction

Solution-processable polymer solar cells (PSCs) have received substantial consideration as a renewable energy source due to their benefits such as being flexible devices, light weight, low costs, and easy fabrication [1–4]. The most successful method to build an active layer of PSCs is based on the

bulk heterojunction (BHJ) architecture [5,6]. The photoactive layer is comprised of a phase-separated blend of a polymer donor and a fullerene acceptor. To achieve high power-conversion efficiencies (PCEs) with these devices, the conjugated polymer should have a low-lying HOMO level to obtain high open circuit voltage (V_{oc}) value, a low optical band gap to ensure high short circuit current density (J_{sc}) value, a high absorption coefficient, and a good hole mobility [7,8]. The most efficient strategy to construct narrow-band-gap polymers relies on the use of alternating donor (D) and acceptor (A) moieties along the backbone of conjugated polymers. Using this strategy, several kinds of D-A copolymers have shown excellent PCEs and reaching up to 17% [9]. A range of electron-donating monomers have been successfully developed for use in this area such as fluorene, carbazole, dibenzosilole (DBS), anthracene, cyclopentadithiophene (CPDT), dithienosilole (DTS), and benzodithiophene (BDT). In addition, many types of electron-accepting building blocks such as benzothiadiazole (BT), diketopyrrolopyrrole (DPP), quinoxaline (Q), and thienopyrroledione (TPD) have been used in D-A copolymers.

One of the most studied electron-accepting (A) heterocycles is the benzothiadiazole moiety [10]. Two types of comonomers have been developed for photovoltaic materials. The first one is the use of 2,1,3-benzothiadiazole (BT) which can be copolymerized with a variety of electron-donating (D) moieties to construct push-pull narrow-band-gap conjugated polymers for BHJ photovoltaic cells [11,12]. The second comonomer is the 4,7-di-2-thienyl-2,1,3-benzothiadiazole (DTBT), where there are two flanking thienyl units between the BT moiety and the electron-donating unit [13–15]. The advantages of these two thiophene spacers are to reduce the steric hindrance so that the resulting D-A copolymers adopt more planar structures [16]. In addition, these polymers possess higher charge carrier (usually hole) mobility and low band gaps [17]. However, the copolymers based on DTBT units have poor solubilities and have low molecular weights. The donor units must contain solubilizing groups of sufficient bulk to enable processability of the polymers [18]. To address this issue, 5,6-positions of the BT unit can be used for anchoring either electron-releasing or electron-accepting substituents in order to increase solubility, molecular weights and tuning the HOMO and LUMO levels of the resulting copolymers [19,20]. By attaching alkoxy chains on these positions, two weaker electron-accepting units called 5,6-dialkoxy-2,1,3-benzothiadiazole [(OR)₂BT] and 4,7-di-2-thienyl-5,6-dialkoxy-2,1,3-benzothiadiazole [DT(OR)₂BT] emerged [21]. Polymers containing these new acceptor repeat units have higher solubilities than polymers containing unsubstituted BT. However, by adding two electron-withdrawing substituents such as fluorine atoms, another new acceptor unit of 4,7-di-2-thienyl-5,6-difluoro-2,1,3-benzothiadiazole (DTffBT) emerged [22]. This fluorinated BT monomer is stronger electron-acceptor unit than BT with deeper HOMO and LUMO energy levels which lead to higher V_{oc} value compared to DTBT analogue. Several copolymers with high PCEs were reported based on DTffBT [22]. Recently, a new acceptor moiety 4,7-di-2-thienyl-2,1,3-benzothiadiazole-5,6-*N*-alkyl-dicarboxylic imide (DTBTDI), which consists of the dicarboxylic imide group fused to the BT unit has been developed [20,23,24]. This acceptor has been shown as a stronger electron-deficient unit compared to both DTBT and DTffBT analogues.

In 2013, Wang et al. synthesized two novel copolymers based on DTBTDI and benzodithiophene units which were used for solar cell applications [23]. These polymers were prepared by the Stille polymerization between dibrominated DTBTDI and distannylated benzodithiophene monomers. Both PDI-BDTT and PDI-BDTO polymers have the same side chain on the acceptor unit and different side chains attached to the 4,8-positions of benzodithiophene units. The solar cell based on a PDI-BDTT:PC₇₁BM delivered an impressive PCE of 5.19%. In contrast, under the same experimental conditions, PDI-BDTO:PC₇₁BM showed a lower PCE of 2.10% [23].

More recently, Li et al. synthesized two other polymers based on the same acceptor, with benzodithiophene and dithienyl fluorene (DTF) as donors units [24]. The polymers P(BTI-B) and P(BTI-F) were synthesized by the Stille polymerization between dibrominated DTBTDI and distannylated BDT and DTF units. BHJ photovoltaic cells fabricated from P(BTI-B):PC₆₁BM and P(BTI-F):PC₆₁BM offered a PCE of 3.42 and 1.61%, respectively.

Lately, Nielsen and co-workers prepared two novel copolymers based on the same acceptor and benzotrithiophene (BTT) as donor unit [20]. The polymers, BBTI-1 and BBTI-2, were prepared

by microwave Stille coupling polymerization between dibrominated DTBTDI with distannylated BTT. The BHJ photovoltaic cells including BBTI-1:PC₇₁BM gave a remarkable PCE of 8.3%. However, BBTI-2:PC₇₁BM delivered a lower PCE of 6%.

Polyfluorene (PF) and their derivatives, which belong to the class of materials with fused ring aromatic systems, are rigid and provide coplanar backbone. PF derivatives generally possess low HOMO energy levels around -5.5 eV, which makes them thermally and chemically stable. Due to their good solubility and high photoluminescence efficiency, conjugated polymers containing fluorene units have been widely investigated as blue emissive materials for organic light emitting diode (OLED) applications.

Fluorene unit is one of the promising donor building blocks for solar cell applications owing to the low HOMO energy levels and acceptable hole mobilities of PF derivatives, which provide high V_{oc} values and moderate J_{sc} values in organic photovoltaic (OPV) devices. However, PFs have large band gaps (2.8–3.0 eV) and they are not suitable for efficient OPVs. This problem can be addressed by incorporating acceptor units into polymer backbones to generate alternating D-A copolymers, which lower the band gaps to efficiently harvest sunlight.

The D-A copolymers based on fluorene as the donor units with various acceptor units such as DTBT [18], quinoxaline (Q) [25], thienopyrazine (TP) [26] and pyrazinoquinoxaline (PQ) [27] were reported. The poly[2,7-(9-(2'-ethylhexyl)-9-hexyl-fluorene)-*alt*-5,5'-(4',7'-di-2-thienyl-2',1',3'-benzothiadiazole)] (PFDTBT) was the first D-A copolymer synthesized by Suzuki polymerization and published by Andersson and co-workers with an optical band gap (~ 1.9 eV) and with poor solubility [18]. When the polymer was blended with PC₆₁BM as the electron acceptor, the photovoltaic performance of the resulting polymer was 2.2%. A similar polymer PF8DTBT with two *n*-octyl chains in the 9-position of fluorene units exhibited a slightly higher PCE of 2.84% [28]. Slooff et al. reported the same polymer backbone with two *n*-decyl chains on the fluorene moiety, PF10DTBT [15]. The PCE of 4.2% was obtained for PF10DTBT:PC₆₁BM based photovoltaic cell. Later on, linear alkyl chains substituted with 3,7-dimethyloctyl side chains (DMO) to generate a new polymer, BisDMO-PFDTBT [14]. The BisDMO-PFDTBT was used in photovoltaic cell with PC₇₁BM as the acceptor, showed higher PCE of 4.5%.

Iraqi et al. designed and synthesized four copolymers based on 2,7-fluorene and BT with or without octyloxy substituents [29]. In addition, two flanked thiophene or selenophene units are incorporated between donor and acceptor moieties. All polymers were prepared by Suzuki polymerization. The polymers were fabricated with PC₇₁BM in BHJ devices gave PCE between 3.45 and 5.41%. Iraqi and co-workers further reported a novel copolymer PFDT2BT-8 based on 2,7-fluorene with (OR)₂ BT [30]. In addition, two bithiophene units as spacers are inserted between donor and acceptor moieties. PFDT2BT-8 was synthesized by Suzuki polymerization. BHJ devices based on PFDT2BT-8:PC₇₁BM gave an impressive PCE of 6.20%. PFDTTBT-8 was developed and synthesized by Iraqi et al. using two thieno[3,2-*b*]thiophene (TT) units as spacers between 2,7-fluorene and (OR)₂ BT [31]. PFDTTBT-8:PC₇₁BM gave a PCE of 4.43%.

Gadisa and co-workers reported an alternating D-A copolymer, APFO-15 based on fluorene as a donor unit and dithienylquinoxaline (TQT) as acceptor unit [25,32]. The BHJ PSCs based on APFO-15:PC₆₁BM showed a PCE of 3.7%. Kitazawa et al. reported the same polymer backbone PFTQT but without octyloxy groups on the phenyl rings of the quinoxaline unit [33]. The PFTQT:PC₇₁BM gave a higher PCE of 5.5%. By replacing the benzothiadiazole and quinoxaline by thienopyrazine (TP) as a unit a new D-A copolymer, APFO-Green5 was reported by Zhang and co-workers [26,32]. APFO-Green5 devices fabricated with PC₆₁BM delivered a moderate PCE of 2.2%. TP unit was replaced by pyrazinoquinoxaline (PQ) unit and yielded APFO-Green9. The PSCs based on APFO-Green9:PC₇₁BM achieved a PCE of 2.3% [27].

Upon introduction of a silicon atom instead of a methylene bridge in fluorene, which is another promising donor unit dibenzosilole (DBS) has emerged. Leclerc et al. were the first research group to prepare a D-A copolymer, poly[9,9-dioctyl-2,7-dibenzosilole-*alt*-5,5'-(4',7'-di-2-thienyl-2',1',3'-benzothiadiazole)] (PDBSDTBT) based on DBS and DTBT for photovoltaic applications [34].

The photovoltaic performance of this polymer with PC₆₁BM as the acceptor delivered a PCE of 1.6%. Soon after, Cao et al. independently reported a higher PCE of 5.4% for the same polymer using 4-fold higher M_n (79,000 g·mol⁻¹) [35]. The improved performance of PDBSDTBT compared to PFDTBT analogue was due to higher hole mobility measured by FET and broader absorption spectrum. In addition, the C-Si bond in DBS unit is longer than C-C bond in fluorene unit. Consequently, DBS units create less steric hindrance compared to their fluorene counterparts and therefore a better π - π stacking between polymer chains is expected [36].

In this work, we reported the synthesis of four fluorene and dibenzosilole-based copolymers by copolymerizing 2,7-fluorene and 2,7-dibenzosilole (DBS) with both 4,7-di(5-bromo-thien-2-yl)-2,1,3-benzothiadiazole-5,6-*N*-(3,7-dimethyloctyl)dicarboxylic imide (M1) and 4,7-di(5-bromo-thien-2-yl)-2,1,3-benzothiadiazole-5,6-*N*-octyl-dicarboxylic imide (M2) and yielded PFDTBTDI-DMO, PFDTBTDI-8, PDBSDTBTDI-DMO, and PDBSDTBTDI-8, respectively. The prepared polymers were characterized by UV-vis and cyclic voltammetry to determine their energy band gaps.

2. Experimental Section

2.1. Materials

All the starting materials and reagents obtained from Sigma-Aldrich and Alfa Aesar and used without further purification. Most of the reactions were carried out under argon atmosphere. Anhydrous solvents used for the reactions obtained from Grubbs solvent purification system within the Sheffield University/Chemistry Department. All the monomers used for preparing the polymers in this article were synthesized according to the procedure part.

2.2. Measurements

All ¹H NMR and ¹³C NMR nuclear magnetic resonance (NMR) spectra for the monomers measured either with a Bruker Avance AV 3HD 400 (400 MHz) spectrometer in deuterated chloroform (CDCl₃), deuterated acetone (CD₃COCD₃) or deuterated dimethyl sulfoxide (CD₃SOCD₃) as the solvents at room temperature. The ¹H NMR spectra for the polymers were measured with Bruker AV 3HD 500 (500 MHz) in deuterated 1,1,2,2-tetrachloroethane (C₂D₂Cl₄) as the solvent at 100 °C. The chemical shifts were measured in parts per million (ppm). The coupling constants (*J*) are calculated in Hertz (Hz). The ¹H NMR and ¹³C NMR spectra were analyzed using Bruker TopSpin 3.2 software. Elemental analysis (CHN) was performed by either the Perkin Elmer 2400 CHNS/O Series II Elemental Analyzer or Vario MICRO Cube CHN/S Elemental Analyzer for CHN analysis. Anion analysis (Br, I, and S) was performed by the Schöniger oxygen flask combustion method. Mass spectra for the monomers were recorded on Agilent 7200 accurate mass Q-TOF GC-MS spectrometer. Helium is used as a carrier gas in rate of (1.2 mL·min⁻¹), the injection volume is (1.0 μ L) and the concentration of measured sample is (5 mg·mL⁻¹) in CHCl₃ solvent. The temperature program is between 60 to 320 °C at 10 °C·min⁻¹. Mass spectra for the monomers were obtained by the electron ionization method (EI). Gel permeation chromatography (GPC) measurements accomplished by Viscotek GPC Max, a waters 410 instrument with a differential refractive index detector, two polymer labs PLgel 5 μ Mixed C (7.5 \times 300 mm) columns and a guard (7.5 \times 50 mm). Molecular weights for the polymers were determined by preparing polymer solutions (2.5 mg·mL⁻¹) using HPLC grade CHCl₃. The columns were thermostated at 40 °C using CHCl₃. UV-vis absorption spectra were measured by SPECORD S600 UV/visible Spectrophotometer at room temperature. The absorbance of the polymers was measured in CHCl₃ solution using quartz cuvettes (light path length = 10 mm) and blank quartz cuvettes including CHCl₃ was used as a reference. The polymers were coated on quartz substrates from CHCl₃ solutions (1 mg·mL⁻¹) and blank quartz substrate was used as a reference. Thermogravimetric analysis (TGA) measurements were recorded by Perkin Elmer (Pyris 1) thermogravimetric Analyzer. Platinum pans were used as sample holder and the weight of the measured samples was about (3 mg). Cyclic voltammograms were measured using a Model 263A Potentiostat/Galvanostat-Princeton Applied Research. A standard

three electrode system was used based on a Pt disk working electrode, a silver wire reference electrode (Ag/Ag^+) inserted in (0.01 M) AgNO_3 solution in acetonitrile and put it in the electrolyte solution and a Pt wire counter electrode was purged with argon atmosphere during all measurements at room temperature. Tetrabutylammonium perchlorate in acetonitrile ($\text{Bu}_4\text{NClO}_4/\text{CH}_3\text{CN}$) (0.1 M) was used as the electrolyte. Polymer thin films were drop cast onto the Pt disk from polymer solutions in CH_2Cl_2 ($1 \text{ mg}\cdot\text{mL}^{-1}$) and dried under nitrogen prior to measurement. Ferrocene (Fc/Fc^+) was used as a reference redox system. Powder X-ray diffraction (XRD) for the polymers was measured by Bruker D8 ADVANCE X-ray powder diffractometer. Infrared absorption spectra recorded on ATR Perkin Elmer Rx/FT-IR system and Nicolet Model 205 FT-IR spectrometer.

2.3. Monomers and Polymers Synthesis

2.3.1. Synthesis of 2,5-dibromothiophene (1)

Thiophene (25.00 g, 297.12 mmol) in DMF (250 mL) added to a flask and cooled to -15°C . To this solution, NBS (110.00 g, 618.04 mmol) in DMF (300 mL) was added dropwise in the dark and the reaction stirred overnight at RT. The reaction contents were put into ice and DCM and subsequently extracted with DCM and the organic phase washed with deionized H_2O to a neutral pH. The organic layer was collected and dried over MgSO_4 and the solvent concentrated to afford the product which purified by vacuum distillation and gave 1 as a yellow oil (59.30 g, 245 mmol, 82% yield) [37]. ^1H NMR (CDCl_3 , δ): 6.87 (s, 2H). ^{13}C NMR (CDCl_3 , δ): 130.4, 111.6. FT-IR (cm^{-1}): 3096, 1726, 1516, 1410, 1200. EI-MS (m/z): 242 $[\text{M}]^+$. EA (%) calculated for $\text{C}_4\text{H}_2\text{Br}_2\text{S}$: C, 19.86; H, 0.83; Br, 66.06, S, 13.25. Found: C, 20.01; H, 0.85; Br, 65.02, S, 11.96.

2.3.2. Synthesis of 2,5-dibromo-3,4-dinitrothiophene (2)

Concentrated H_2SO_4 (150 mL) and fuming H_2SO_4 (150 mL, 20% free SO_3) combined in a flask. This flask was cooled to 0°C and 1 (26.00 g, 107.46 mmol) was added dropwise. Concentrated nitric acid (125 mL) was added dropwise and the reaction contents kept under 20°C . During addition of nitric acid yellow precipitate formed quickly. The mixture was stirred for 3 h at $20\text{--}30^\circ\text{C}$. Then, the mixture was poured into ice and upon melting of the ice a yellow precipitate filtrated and washed thoroughly with deionized H_2O . The product recrystallized from methanol to afford 2 as yellow crystals (32.50 g, 98 mmol, 91% yield) [38]. ^{13}C NMR (CDCl_3 , δ): 140.7, 113.4. FT-IR (cm^{-1}): 2886, 2851, 2813, 1535, 1497, 1345, 1081. EI-MS (m/z): 332 $[\text{M}]^+$. EA (%) calculated for $\text{C}_4\text{Br}_2\text{N}_2\text{O}_4\text{S}$: C, 14.47; N, 8.44; S, 9.66; Br, 48.15. Found: C, 14.51; N, 7.91; S, 9.19; Br, 46.57.

2.3.3. Synthesis of 3',4'-dinitro-2,2':5,2''-terthiophene (3)

In a flask, 2 (9.90 g, 29.82 mmol), 2-(tributylstannyl)thiophene (27.82 g, 74.54 mmol) and $\text{PdCl}_2(\text{PPh}_3)_2$ (0.45 g, 0.64 mmol) added. The system was degassed under argon and anhydrous toluene (100 mL) added and heated at 115°C for 24 h. The flask was cooled to RT and the volatiles removed to obtain the product which purified by column chromatography with gradient (petroleum ether, 0–50% DCM) to obtain an orange solid and the product further purified by recrystallization from methanol to afford 3 as orange crystals (9.10 g, 27 mmol, 90% yield) [39]. ^1H NMR (CDCl_3 , δ): 7.62 (dd, 2H, $J = 1.0 \text{ Hz}$, 5.0 Hz), 7.56 (dd, 2H, $J = 1.0 \text{ Hz}$, 4.0 Hz), 7.19 (dd, 2H, $J = 4.0 \text{ Hz}$, 5.0 Hz). ^{13}C NMR (CDCl_3 , δ): 135.9, 133.9, 131.3, 131.2, 128.4, 128.0. FT-IR (cm^{-1}): 3076, 1821, 1528, 1379, 1348, 1299, 1223, 1066. EI-MS (m/z): 338 $[\text{M}]^+$. EA (%) calculated for $\text{C}_{12}\text{H}_6\text{N}_2\text{O}_4\text{S}_3$: C, 42.60; H, 1.79; N, 8.28; S, 28.42. Found: C, 42.49; H, 1.66; N, 8.13; S, 28.16.

2.3.4. Synthesis of 3',4'-diamino-2,2':5,2''-terthiophene (4)

EtOH (31 mL) and HCl (62 mL, 35%) added to 3 (3.00 g, 8.86 mmol) in a flask. To this mixture, anhydrous tin (II) chloride (31.00 g, 163.50 mmol) in ethanol (62 mL) was added and stirred at 30°C for 24 h. The mixture was cooled to RT and put into cold NaOH . To this mixture, toluene was added and

then stirred vigorously and filtered through celite. The product was extracted with toluene and the organic phases washed with NaCl and subsequently dried over MgSO₄. The solvent was concentrated to obtain the 4 as a brown solid (2.40 g, 9 mmol, 97% yield) [40]. ¹H NMR (CDCl₃, δ): 7.30 (d, 2H, J = 2.0 Hz), 7.27 (s, 2H), 7.09–7.14 (m, 2H), 3.76 (bs, 4H). ¹³C NMR (CDCl₃, δ): 136.0, 133.6, 127.8, 124.0, 124.0, 110.1. FT-IR (cm⁻¹): 3371, 3298, 3224, 3182, 3096, 1631, 1615, 1573, 1528, 1509, 1441, 1336, 1294, 1070. EI-MS (*m/z*): 278 [M]⁺. EA (%) calculated for C₁₂H₁₀N₂S₃: C, 51.77; H, 3.62; N, 10.06; S, 34.55. Found: C, 51.69; H, 3.54; N, 9.97; S, 34.78.

2.3.5. Synthesis of 4,6-bis(2-thienyl)-thieno[3,4-c][1,2,5]-thiadiazole (5)

4 (1.67 g, 5.99 mmol) dissolved in dry pyridine (30 mL) in a flask and degassed under argon. To this mixture, *N*-thionylaniline (1.60 g, 11.49 mmol) was added drop wise and chlorotrimethylsilane (4.50 g, 41.42 mmol) then added drop wise, resulting in a dark blue color. The reaction contents were stirred for 3 h at RT and then put into DCM. The solution was washed with HCl and with deionized water and extracted with DCM. The organic phase was dried over anhydrous MgSO₄ and subsequently filtered. The solvent was evaporated to afford the product which purified via chromatography with DCM to afford 5 as blue crystals (1.72 g, 6 mmol, 93% yield) [41]. ¹H NMR (CDCl₃, δ): 7.59 (dd, 2H, J = 1.0 Hz, 3.5 Hz), 7.34 (dd, 2H, J = 1.0 Hz, 5.0 Hz), 7.12 (dd, 2H, J = 3.5 Hz, 5.0 Hz). ¹³C NMR (CDCl₃, δ): 156.3, 135.0, 128.2, 125.4, 124.3, 112.4. FT-IR (cm⁻¹): 3102, 3073, 1797, 1525, 1483, 1365, 1223, 1137, 1047. EI-MS (*m/z*): 306 [M]⁺. EA (%) calculated for C₁₂H₆N₂S₄: C, 47.04; H, 1.97; N, 9.14; S, 41.85. Found: C, 47.25; H, 2.18; N, 8.83; S, 39.16.

2.3.6. Synthesis of 4,7-di(thien-2-yl)-2,1,3-benzothiadiazole-5,6-dimethyl Ester (6)

5 (1.86 g, 6.06 mmol) and dimethyl acetylenedicarboxylate (1.73 g, 12.17 mmol) was combined in a flask. The system was evacuated and refilled with argon for three cycles before anhydrous xylene (40 mL) added. The reaction contents were refluxed for 24 h. The flask was cooled to RT and the solvent removed to afford the product which was purified by column chromatography with gradient (petroleum ether, 0–50% DCM) to afford 6 as yellow crystals (2.37 g, 6 mmol, 94% yield) [23]. ¹H NMR (CDCl₃, δ): 7.62 (dd, 2H, J = 1.0 Hz, 5.0 Hz), 7.44 (dd, 2H, J = 1.0 Hz, 3.5 Hz), 7.22 (dd, 2H, J = 3.5 Hz, 5.0 Hz), 3.78 (s, 6H). ¹³C NMR (CDCl₃, δ): 168.1, 153.6, 135.1, 132.0, 129.7, 129.0, 127.3, 126.2, 53.1. FT-IR (cm⁻¹): 3109, 2975, 2932, 2900, 2865, 2159, 2031, 1971, 1730, 1513, 1460, 1318, 1283, 1198. EI-MS (*m/z*): 416 [M]⁺. EA (%) calculated for C₁₈H₁₂N₂O₄S₃: C, 51.91; H, 2.90; N, 6.73; S, 23.09. Found: C, 51.86; H, 2.94; N, 6.61; S, 22.97.

2.3.7. Synthesis of 4,7-di(thien-2-yl)-2,1,3-benzothiadiazole-5,6-dicarboxylic Acid (7)

Sodium hydroxide (4.00 g, 100.00 mmol) was dissolved in deionized water (30 mL) and added to a flask. To this solution, ethanol (200 mL) and 6 (2.27 g, 5.45 mmol) was added and the reaction contents refluxed for 24 h. The flask was cooled to RT and deionized H₂O added. This mixture was cooled to 0 °C and neutralized by HCl to precipitate the product. The precipitate was filtered and subsequently washed with deionized H₂O. The precipitate was dried under high vacuum to afford 7 as yellow solid (1.80 g, 5 mmol, 85% yield) [20]. ¹H NMR (CD₃SOCD₃, δ): 7.86 (dd, 2H, J = 1.0 Hz, 5.0 Hz), 7.47 (dd, 2H, J = 1.0 Hz, 3.5 Hz), 7.25 (dd, 2H, J = 3.5 Hz, 5.0 Hz). ¹³C NMR (CD₃SOCD₃, δ): 168.4, 152.5, 134.8, 133.0, 129.7, 129.3, 127.2, 123.8. FT-IR (cm⁻¹): 3106, broad (3300–2600), 2162, 2024, 1971, 1815, 1765, 1705, 1552, 1453, 1386, 1261, 1152, 1020. EI-MS (*m/z*): 387 [M-H]⁺. EA (%) calculated for C₁₆H₈N₂O₄S₃: C, 49.48; H, 2.08; N, 7.21; S, 24.76. Found: C, 45.33; H, 2.70; N, 6.47; S, 21.35.

2.3.8. Synthesis of 4,7-di(thien-2-yl)-2,1,3-benzothiadiazole-5,6-dicarboxylic Anhydride (8)

7 (1.15 g, 2.96 mmol) and anhydrous acetic anhydride (10.00 g, 97.95 mmol) combined in a flask. The system was evacuated and refilled with argon for three cycles before anhydrous xylene (30 mL) added. The mixture was heated at 130 °C for 6 h. The mixture was cooled to RT, and the solvent evaporated to obtain 8 as red solid (1.06 g, 3 mmol, 97% yield) [42]. ¹H NMR (CDCl₃, δ): 8.11 (dd,

2H, $J = 1.0$ Hz, 4.0 Hz), 7.82 (dd, 2H, $J = 1.0$ Hz, 5.0 Hz), 7.33 (dd, 2H, $J = 4.0$ Hz, 5.0 Hz). ^{13}C NMR (CD_3SOCD_3 , δ): 162.0, 156.0, 134.3, 132.6, 131.4, 127.8, 127.6, 125.5. FT-IR (cm^{-1}): 3131, 3109, 3081, 1808, 1765, 1552, 1453, 1393, 1247, 1152, 1088. EI-MS (m/z): 370 $[\text{M}]^+$. EA (%) calculated for $\text{C}_{16}\text{H}_6\text{N}_2\text{O}_3\text{S}_3$: C, 51.88; H, 1.63; N, 7.56; S, 25.97. Found: C, 52.11; H, 2.00; N, 7.20; S, 24.55.

2.3.9. Synthesis of 3,7-dimethyloctyl Bromide (9)

Triphenylphosphine (21.10 g, 80.44 mmol) was added to a mixture of 3,7-dimethyloctyl alcohol (12.61 g, 79.69 mmol) and dichloromethane (250 mL) and stirred in a flask. To this mixture, NBS (14.26 g, 80.14 mmol) was added portionwise and stirred at RT for 90 min. The mixture was washed with NaHCO_3 solution, dried over MgSO_4 , filtered, and the solvent evaporated. The substance was stirred in petroleum ether for 1 h at RT, filtered and the filtrate evaporated. The product was purified by chromatography with petroleum ether to yield 9 as colorless oil (23.00 g, 59 mmol, 73% yield) [43]. ^1H NMR (CDCl_3 , δ): 3.55–3.37 (m, 2H), 1.96–1.83 (m, 1H), 1.77–1.61 (m, 2H), 1.60–1.49 (m, 1H), 1.41–1.24 (m, 3H), 1.22–1.11 (m, 3H), 0.82–0.94 (m, 9H). ^{13}C NMR (CDCl_3 , δ): 40.1, 39.2, 36.7, 32.3, 31.7, 28.0, 24.6, 22.7, 22.6, 19.0. FT-IR (cm^{-1}): 2953, 2925, 2868, 1464, 1382, 1261, 1173. EI-MS (m/z): 222.1 $[\text{M}]^+$. EA (%) calculated for $\text{C}_{10}\text{H}_{21}\text{Br}$: C, 54.30; H, 9.57; Br, 36.13. Found: C, 55.04; H, 9.53; Br, 34.23.

2.3.10. Synthesis of N-(3,7-dimethyloctyl)phthalimide (10)

9 (4.07 g, 18.40 mmol) and anhydrous DMF (20 mL) added into a flask. To this mixture, potassium phthalimide (3.75 g, 20.27 mmol) was added and the reaction contents heated to 90 °C for 17 h. The mixture was cooled to RT and put in deionized H_2O and the product subsequently extracted with DCM. The organic extracts were combined, washed with KOH and deionized water. The organic phase was dried over MgSO_4 and the solvent was evaporated to obtain the product which was purified via chromatography with dichloromethane to yield 10 as colorless oil (5.29 g, 18 mmol, 91% yield) [44]. ^1H NMR (CDCl_3 , δ): 7.85 (dd, 2H, $J = 3.0$ Hz, 5.5 Hz), 7.72 (dd, 2H, $J = 3.0$ Hz, 5.5 Hz), 3.80–3.66 (m, 2H), 1.77–1.66 (m, 1H), 1.53–1.43 (m, 3H), 1.41–1.25 (m, 3H), 1.20–1.11 (m, 3H), 0.98 (d, 3H, $J = 6.5$ Hz), 0.87 (d, 6H, $J = 7.0$ Hz). ^{13}C NMR (CDCl_3 , δ): 168.4, 133.8, 132.2, 123.1, 39.2, 37.0, 36.3, 35.5, 30.7, 27.9, 24.5, 22.7, 22.6, 19.4. FT-IR (cm^{-1}): 2953, 2925, 2868, 1772, 1706, 1616, 1469, 1398, 1267, 1189, 1055. EI-MS (m/z): 288.2 $[\text{MH}]^+$. EA (%) calculated for $\text{C}_{18}\text{H}_{25}\text{NO}_2$: C, 75.22; H, 8.77; N, 4.87. Found: C, 72.17; H, 8.62; N, 4.43.

2.3.11. Synthesis of 3,7-dimethyl-1-octanamine (11)

10 (6.03 g, 20.98 mmol), hydrazine hydrate (4.0 mL, 65.0 mmol, 51%) and methanol (100 mL) were combined in a flask. The reaction contents were refluxed until the starting material disappeared. Upon completion, excess HCl was added and the mixture refluxed for 1 h and then cooled to RT. The precipitate was filtered and washed with water. The methanol was concentrated and the residue diluted with dichloromethane. The organic layer was washed with KOH and the product extracted with dichloromethane. The organic phase was washed with NaCl, dried over MgSO_4 and the solvent was concentrated to yield 11 as a brown oil (2.85 g, 18 mmol, 86% yield) [45]. ^1H NMR (CDCl_3 , δ): 2.82–2.62 (m, 2H), 1.60–1.43 (m, 3H), 1.35–1.22 (m, 4H), 1.20–1.06 (m, 3H), 0.88 (dd, 9H, $J = 2.0$ Hz, 6.5 Hz). ^{13}C NMR (CDCl_3 , δ): 41.1, 40.1, 39.3, 37.3, 30.5, 28.0, 24.7, 22.7, 22.6, 19.6. FT-IR (cm^{-1}): 3521, 3375, 3219, 3021, 2953, 2925, 2868, 2155, 2028, 1978, 1598, 1464, 1382, 1166, 1063. EI-MS (m/z): 157.2 $[\text{M}]^+$. EA (%) calculated for $\text{C}_{10}\text{H}_{23}\text{N}$: C, 76.36; H, 14.74; N, 8.90. Found: C, 71.74; H, 13.51; N, 7.71.

2.3.12. Synthesis of 4,7-di(thien-2-yl)-2,1,3-benzothiadiazole-5,6-N-(3,7-dimethyloctyl)dicarboxylic Imide (12)

8 (1.00 g, 2.69 mmol), acetic acid (50 mL, 100%) and 11 (0.88 g, 5.59 mmol) was combined in a flask. The system was evacuated and refilled with argon for three cycles and heated at 110 °C overnight. The mixture was cooled to RT, acetic anhydride (20 mL) added and heated at 110 °C for 6 h. The mixture was cooled to RT and the solvent concentrated to yield the product which was purified by

chromatography with (60:10, petroleum ether: ethyl acetate) to afford 12 as an orange solid (1.15 g, 2.3 mmol, 84% yield) [42]. $^1\text{H NMR}$ (CDCl_3 , δ): 7.91 (dd, 2H, $J = 1.0$ Hz, 3.5 Hz), 7.73 (dd, 2H, $J = 1.0$ Hz, 5.0 Hz), 7.30 (dd, 2H, $J = 3.5$ Hz, 5.0 Hz), 3.84–3.70 (m, 2H), 1.78–1.65 (m, 1H), 1.55–1.43 (m, 3H), 1.39–1.22 (m, 3H), 1.20–1.08 (m, 3H), 0.97 (d, 3H, $J = 6.0$ Hz), 0.86 (d, 6H, $J = 6.0$ Hz). $^{13}\text{C NMR}$ (CDCl_3 , δ): 165.7, 156.5, 133.1, 131.5, 130.2, 127.0, 126.9, 126.7, 39.2, 37.2, 37.0, 35.2, 31.0, 27.9, 24.6, 22.7, 22.6, 19.4. FT-IR (cm^{-1}): 3439, 3102, 3074, 2953, 2925, 2865, 1804, 1751, 1694, 1549, 1453, 1364, 1226, 1162, 1056. EI-MS (m/z): 510.1 $[\text{MH}]^+$. EA (%) calculated for $\text{C}_{26}\text{H}_{27}\text{N}_3\text{O}_2\text{S}_3$: C, 61.27; H, 5.34; N, 8.24; S, 18.87. Found: C, 61.59; H, 5.56; N, 7.94; S, 16.79.

2.3.13. Synthesis of 4,7-di(thien-2-yl)-2,1,3-benzothiadiazole-5,6-N-octyl-dicarboxylic imide (13)

13 was prepared followed by the same procedure for synthesis of 12 except N-octylamine (1.20 g, 9.28 mmol) was used. 13 was obtained as an orange solid (1.20 g, 2.5 mmol, 93% yield) [42]. $^1\text{H NMR}$ (CDCl_3 , δ): 7.91 (dd, 2H, $J = 1.0$ Hz, 3.5 Hz), 7.73 (dd, 2H, $J = 1.0$ Hz, 5.0 Hz), 7.30 (dd, 2H, $J = 3.5$ Hz, 5.0 Hz), 3.74 (t, 2H, $J = 7.5$ Hz), 1.65–1.76 (m, 2H), 1.23–1.41 (m, 10H), 0.88 (t, 3H, $J = 7.0$ Hz). $^{13}\text{C NMR}$ (CDCl_3 , δ): 165.8, 156.5, 133.1, 131.5, 130.2, 127.1, 126.9, 126.7, 39.0, 31.8, 29.1, 28.2, 27.0, 22.7, 14.0. FT-IR (cm^{-1}): 3443, 3102, 3070, 2918, 2854, 1808, 1754, 1694, 1556, 1457, 1364, 1226, 1169, 1098. EI-MS (m/z): 481.1 $[\text{M}]^+$. EA (%) calculated for $\text{C}_{24}\text{H}_{23}\text{N}_3\text{O}_2\text{S}_3$: C, 59.85; H, 4.81; N, 8.72; S, 19.97. Found: C, 59.91; H, 4.93; N, 8.70; S, 20.72.

2.3.14. Synthesis of 4,7-di(5-bromo-thien-2-yl)-2,1,3-benzothiadiazole-5,6-N-(3,7-dimethyloctyl) Dicarboxylic Imide (M1)

12 (1.00 g, 1.96 mmol) and THF (100 mL) was combined in a flask. To this mixture, NBS (1.74 g, 9.77 mmol) was added and stirred at RT overnight in the dark. The solvent was evaporated to obtain the product as red solid, subsequently washed with cold CH_3OH , filtered and dried. The product was purified via chromatography with DCM to yield M1 as red solid (1.28 g, 2 mmol, 98% yield) [20]. $^1\text{H NMR}$ (CDCl_3 , δ): 7.80 (d, 2H, $J = 4.0$ Hz), 7.24 (d, 2H, $J = 4.0$ Hz), 3.70–3.84 (m, 2H), 1.78–1.66 (m, 1H), 1.54–1.44 (m, 3H), 1.41–1.22 (m, 3H), 1.20–1.11 (m, 3H), 0.98 (d, 3H, $J = 6.0$ Hz), 0.87 (d, 6H, $J = 6.5$ Hz). $^{13}\text{C NMR}$ (CDCl_3 , δ): 165.6, 155.9, 134.1, 133.0, 129.8, 126.4, 125.8, 118.7, 39.2, 37.3, 37.0, 35.2, 31.0, 27.9, 24.6, 22.7, 22.6, 19.4. FT-IR (cm^{-1}): 3429, 3120, 2957, 2918, 2865, 1747, 1691, 1563, 1460, 1364, 1283, 1073. EI-MS (m/z): 666.9 $[\text{M}]^+$. EA (%) calculated for $\text{C}_{26}\text{H}_{25}\text{Br}_2\text{N}_3\text{O}_2\text{S}_3$: C, 46.78; H, 3.78; Br, 23.94; N, 6.30; S, 14.41. Found: C, 46.61; H, 3.61; Br, 23.95; N, 6.29; S, 14.64.

2.3.15. Synthesis of 4,7-di(5-bromo-thien-2-yl)-2,1,3-benzothiadiazole-5,6-N-octyl-dicarboxylic Imide (M2)

M2 was prepared followed by the same procedure for synthesis of M1, where compound 13 (1.00 g, 2.07 mmol), used with THF (100 mL) and NBS (1.84 g, 10.33 mmol). M2 was obtained as red solid (1.27 g, 2 mmol, 96% yield) [20]. $^1\text{H NMR}$ (CDCl_3 , δ): 7.80 (d, 2H, $J = 4.0$ Hz), 7.24 (d, 2H, $J = 4.0$ Hz), 3.75 (t, 2H, $J = 7.0$ Hz), 1.66–1.75 (m, 2H), 1.23–1.40 (m, 10H), 0.88 (t, 3H, $J = 6.5$ Hz). $^{13}\text{C NMR}$ (CDCl_3 , δ): 165.7, 156.0, 134.1, 133.0, 129.8, 126.4, 125.9, 118.7, 39.0, 31.8, 29.1, 28.3, 27.0, 22.6, 14.1. FT-IR (cm^{-1}): 3421, 3120, 2953, 2911, 2850, 1744, 1687, 1556, 1446, 1375, 1244, 1176. EI-MS (m/z): 638.9 $[\text{M}]^+$. EA (%) calculated for $\text{C}_{24}\text{H}_{21}\text{Br}_2\text{N}_3\text{O}_2\text{S}_3$: C, 45.08; H, 3.31; N, 6.57; S, 15.04; Br, 24.99. Found: C, 44.79; H, 3.41; N, 6.47; S, 15.74; Br, 28.80.

2.3.16. Synthesis of 4,4'-dibromo-2,2'-dinitrophenyl (14)

2,5-Dibromonitrobenzene (50.00 g, 179.30 mmol) and Cu powder (25.00 g, 393.39 mmol) was combined in a flask. The mixture was evacuated and refilled with argon for three cycles before anhydrous DMF (230 mL) added and heated at 125 °C for 3 h. The reaction contents were cooled to RT and dissolved in toluene and filtered. NaHCO_3 solution was added to the filtrate and the mixture extracted with toluene and the organic phases combined and washed with deionized H_2O numerous times until it became neutral. The organic phase was dried over anhydrous MgSO_4 , filtered and the

solvent evaporated to afford the product which was recrystallized from isopropanol to yield 14 as yellow crystals (32.61 g, 162 mmol, 90% yield) [46]. $^1\text{H NMR}$ (CDCl_3 , δ): 8.40 (d, 2H, $J = 2.0$ Hz), 7.85 (dd, 2H, $J = 2.0$ Hz, 8.0 Hz), 7.18 (d, 2H, $J = 8.0$ Hz). $^{13}\text{C NMR}$ (CDCl_3 , δ): 147.4, 136.6, 132.0, 132.0, 128.1, 123.0. FT-IR (cm^{-1}): 3085, 2847, 1598, 1332, 1276, 1152, 1098. EI-MS (m/z): 403 $[\text{M}]^+$. EA (%) calculated for $\text{C}_{12}\text{H}_6\text{Br}_2\text{N}_2\text{O}_4$: C, 35.85; N, 6.97; Br, 39.75; H, 1.50. Found: C, 35.55; N, 6.77; Br, 39.74; H, 1.59.

2.3.17. Synthesis of 4,4'-dibromobiphenyl-2,2'-diamine (15)

14 (6.00 g, 14.92 mmol), ethanol (74 mL) and HCl (43 mL, 32%) was added to a flask. To this mixture, Sn (7.00 g, 58.96 mmol) was added over 10 min and refluxed for 90 min. The reaction contents were cooled to RT and another portion of Sn (7.00 g, 58.96 mmol) added and refluxed for 90 min. The flask was cooled to RT and the mixture filtered and deionized water added to the filtrate. NaOH solution was added dropwise until pH became approximately 9. The mixture was extracted with Et_2O and organic phase washed with NaCl, dried over MgSO_4 and then filtered. The solvent was concentrated to obtain the 15 as brown crystals (3.58 g, 10.5 mmol, 70% yield) [47]. $^1\text{H NMR}$ (CDCl_3 , δ): 6.99–6.93 (m, 6H), 3.59 (bs, 4H). $^{13}\text{C NMR}$ (CDCl_3 , δ): 145.4, 132.3, 122.7, 122.1, 121.7, 118.2. FT-IR (cm^{-1}): 3393, 3280, 3187, 1630, 1557, 1496, 1396, 1272, 1137, 1081. EI-MS (m/z): 341.9 $[\text{M}]^+$. EA (%) calculated for $\text{C}_{12}\text{H}_{10}\text{Br}_2\text{N}_2$: C, 42.14; N, 8.19; Br, 46.72; H, 2.95. Found: C, 41.74; N, 7.95; Br, 46.71; H, 2.93.

2.3.18. Synthesis of 4,4'-dibromo-2,2'-diiodobiphenyl (16)

15 (5.00 g, 14.61 mmol), HCl (50 mL, 32%), H_2O (200 mL) and acetonitrile (200 mL) were combined in a flask and cooled to 0 °C. To this mixture, NaNO_2 (4.59 g, 66.53 mmol) was dissolved in deionized H_2O (25 mL), added dropwise, and stirred for 1 hour between –5 and –10 °C. KI (22.28 g, 134.21 mmol), dissolved in deionized H_2O (50 mL), and cooled to 0 °C and added dropwise while the reaction temperature maintained at –10 to –15 °C. After addition was completed, the temperature was raised to RT and then heated to 80 °C for 20 h and cooled to RT. The mixture was extracted with DCM, the collected organic layers washed with $\text{Na}_2\text{S}_2\text{O}_3$ solution, deionized water and NaCl solution. The collected organic layers were dried over MgSO_4 , filtered, and the solvent was concentrated to afford the product which was purified via chromatography with petroleum ether. It was further purified by recrystallization from *n*-hexane to yield 16 as white crystals (4.23 g, 7.5 mmol, 51% yield) [48]. $^1\text{H NMR}$ (CDCl_3 , δ): 8.11 (d, 2H, $J = 2.0$ Hz), 7.57 (dd, 2H, $J = 2.0$ Hz, 8.0 Hz), 7.05 (d, 2H, $J = 8.0$ Hz). $^{13}\text{C NMR}$ (CDCl_3 , δ): 146.8, 141.0, 131.4, 130.7, 122.5, 99.9. FT-IR (cm^{-1}): 3400, 3393, 3294, 3191, 1634, 1581, 1449, 1364, 1084. EI-MS (m/z): 563.7 $[\text{M}]^+$. EA (%) calculated for $\text{C}_{12}\text{H}_6\text{Br}_2\text{I}_2$: C, 25.56; H, 1.07; Br, 28.34; I, 45.02. Found: C, 25.47; H, 1.21; Br, 28.14; I, 45.23.

2.3.19. Synthesis of 2,7-dibromo-9,9-dioctyldibenzosilole (17)

16 (4.20 g, 7.44 mmol) was added to a flask. Anhydrous THF (84 mL) was added and the mixture cooled to –78 °C and then the system degassed under argon. To this mixture, *n*-BuLi (12.00 mL, 30.0 mmol) was added dropwise over 2 h. The reaction contents were stirred for 1 h, and dichlorodioctylsilane (4.86 g, 14.95 mmol) was added dropwise over 5 min and the temperature raised to RT and mixture stirred overnight. Deionized water was added, and the product extracted with Et_2O and organic layers collected and washed with brine. The organic layer was dried over MgSO_4 , filtered and the solvent concentrated to yield a product which purified using chromatography with petroleum ether to yield 17 as a colorless oil (3.80 g, 7 mmol, 90% yield) [49]. $^1\text{H NMR}$ (CDCl_3 , δ): 7.70 (d, 2H, $J = 2.0$ Hz), 7.65 (d, 2H, $J = 8.0$ Hz), 7.55 (dd, 2H, $J = 2.0$ Hz, 8.0 Hz), 1.08–1.47 (m, 28H), 0.90 (t, 6H, $J = 2.0$ Hz). $^{13}\text{C NMR}$ (CDCl_3 , δ): 146.0, 140.5, 135.8, 133.1, 122.5, 122.2, 33.2, 31.8, 29.1, 29.0, 23.7, 22.6, 14.1, 11.99. FT-IR (cm^{-1}): 2957, 2921, 2858, 1552, 1446, 1382, 1237, 1141, 1070. EI-MS (m/z): 564.1 $[\text{M}]^+$. EA (%) calculated for $\text{C}_{28}\text{H}_{40}\text{Br}_2\text{Si}$: C, 59.57; H, 7.14; Br, 28.31. Found: C, 60.29; H, 7.60; Br, 24.72%.

2.3.20. Synthesis of 9,9-dioctyl-2,7-bis(4,4,5,5-tetramethyl-1,3,2-dioxaborolan-2-yl)-dibenzosilole (M4)

17 (1.51 g, 2.65 mmol), potassium acetate (1.56 g, 15.89 mmol), bis(pinacolato)diboron (2.36 g, 9.29 mmol) and PdCl₂(dppf) (0.12 g, 0.14 mmol, 5.54 mol%) were combined in a flask and then the system degassed under argon. To this mixture, anhydrous DMF (30 mL) was added and heated at 100 °C for 48 h. The flask was cooled to RT and the product extracted with Et₂O and organic phases washed with deionized H₂O. The organic layers were separated and dried over MgSO₄, filtered and the solvent evaporated to obtain a product which was recrystallized from methanol which passed through the basic alumina to remove the acidic protons to obtain M4 as brown crystals (0.92 g, 1.4 mmol, 53% yield) [50]. ¹H NMR (CDCl₃, δ): 8.07 (s, 2H), 7.92–7.85 (m, 4H), 1.39 (s, 24H), 1.15–1.34 (m, 24H), 0.92–0.99 (m, 4H), 0.86 (t, 6H, J = 7.0 Hz). ¹³C NMR (CDCl₃, δ): 151.0, 139.7, 137.5, 136.8, 120.5, 83.7, 33.4, 31.8, 29.2, 29.0, 24.9, 23.8, 22.6, 14.1, 12.3. FT-IR (cm⁻¹): 2975, 2921, 2854, 1595, 1460, 1343, 1272, 1137, 1091. EI-MS (*m/z*): 658.5 [M]⁺. EA (%) calculated for C₄₀H₆₄B₂O₄Si: C, 72.94; H, 9.79. Found: C, 72.30; H, 9.42.

2.3.21. Synthesis of poly[9,9-dioctyl-2,7-fluorene-alt-5,5-(4',7'-bis(2-thienyl)-2',1',3'-benzothiadiazole-5,6-N-(3,7-dimethyloctyl)dicarboxylic imide)] (PFDTBTDI-DMO)

9,9-Dioctylfluorene-2,7-diboronic acid bis(1,3-propanediol) ester (M3) (125.4 mg, 0.224 mmol) and M1 (150 mg, 0.224 mmol) was added to a flask and degassed under argon. Anhydrous THF (10 mL) was followed by sodium hydrogen carbonate solution (2.5 mL, 5% wt., degassed), added, and the system degassed again. To this mixture, Pd(OAc)₂ (3.7 mg, 0.0168 mmol) and P(*o*-tol)₃ (10.2 mg, 0.0336 mmol) was added, degassed, and heated at 90 °C for 30 h. The flask was cooled to RT, the polymer dissolved in CHCl₃ (200 mL) and an NH₄OH solution (50 mL, 35% in H₂O) added and the mixture stirred overnight. The organic phase was separated and washed with deionized H₂O. The organic phase was concentrated to around (50 mL) and put into methanol (300 mL) and stirred overnight. The mixture was filtered and the polymer cleaned using Soxhlet extraction with methanol (300 mL), acetone (300 mL), hexane (300 mL) and then toluene (300 mL). The toluene fraction was concentrated to around (50 mL) and then put into methanol (300 mL). The mixture was stirred overnight, and the pure polymer was recovered by filtration to afford PFDTBTDI-DMO as purple powders (170 mg, 0.18 mmol, 85% yield) [21]. GPC: toluene fraction, M_n = 16,000 g·mol⁻¹, M_w = 33,000 g·mol⁻¹, PDI = 2.0 and Dp = 18. ¹H NMR (toluene fraction) (C₂D₂Cl₄, δ): 8.02 (d, 2H, J = 3.5 Hz), 7.81–7.68 (bm, 6H), 7.52 (d, 2H, J = 3.5 Hz), 3.90–3.68 (bm, 2H), 2.20–1.99 (bm, 4H), 1.83–1.68 (bm, 1H), 1.61–1.47 (bm, 3H), 1.42–1.34 (bs, 6H), 1.23–1.04 (bm, 24H), 0.99 (d, 3H, J = 6.0 Hz), 0.86 (d, 6H, J = 6.5 Hz), 0.78 (t, 6H, J = 7.0 Hz). FT-IR (cm⁻¹): 2921, 2854, 1754, 1698, 1549, 1364, 1173, 1070. EA (%) calculated for C₅₅H₆₅N₃O₂S₃: C, 73.70; H, 7.31; N, 4.69; S, 10.73. Found: C, 72.52; H, 7.02; N, 4.60; S, 9.38.

2.3.22. Synthesis of poly[9,9-dioctyl-2,7-fluorene-alt-5,5-(4',7'-bis(2-thienyl)-2',1',3'-benzothiadiazole-5,6-N-octyl-dicarboxylic imide)] (PFDTBTDI-8)

PFDTBTDI-8 was prepared followed by the same procedure for synthesis of PFDTBTDI-DMO. M3 (125.4 mg, 0.224 mmol) and M2 (143.2 mg, 0.224 mmol) were copolymerized for 24 h to afford PFDTBTDI-8 as purple powders. Toluene fraction (36 mg, 0.04 mmol, 18% yield), chloroform fraction (120 mg, 0.13 mmol, 60% yield) with total yield 78% [21]. GPC: toluene fraction M_n = 11,200 g·mol⁻¹, M_w = 29,100 g·mol⁻¹, PDI = 2.5 and Dp = 13; chloroform fraction, M_n = 24,900 g·mol⁻¹, M_w = 74,400 g·mol⁻¹, PDI = 2.9 and Dp = 29. ¹H NMR (toluene fraction) (C₂D₂Cl₄, δ): 8.02 (d, 2H, J = 3.5 Hz), 7.81–7.68 (bm, 6H), 7.52 (d, 2H, J = 3.5 Hz), 3.90–3.68 (bm, 2H), 2.20–1.99 (bm, 4H), 1.81–1.71 (bm, 2H), 1.44–1.24 (bm, 10H), 1.23–1.04 (bm, 24H), 0.88 (t, 3H, J = 7.0 Hz), 0.82–0.77 (bm, 6H). FT-IR (cm⁻¹): 2921, 2850, 1754, 1701, 1552, 1400, 1361, 1254, 1166, 1098. EA (%) calculated for C₅₃H₆₁N₃O₂S₃: C, 73.32; H, 7.08; N, 4.84; S, 11.08. Found: C, 72.70; H, 7.02; N, 4.77; S, 10.51.

2.3.23. Synthesis of poly[9,9-dioctyl-2,7-dibenzosilole-alt-5,5-(4',7'-bis(2-thienyl)-2',1',3'-benzothiadiazole-5,6-N-(3,7-dimethyloctyl)dicarboxylic imide)] (PDBSDBTBTDI-DMO)

PDBSDBTBTDI-DMO was prepared followed by the same procedure for synthesis of PFDTBTBTDI-DMO. M4 (147.5 mg, 0.224 mmol) and M1 (150 mg, 0.224 mmol) were copolymerized for 21 h to afford PDBSDBTBTDI-DMO as purple powders. Toluene fraction (50 mg, 0.05 mmol, 22% yield), chloroform fraction (95 mg, 0.10 mmol, 46% yield) with total yield 68% [21]. GPC: toluene fraction, $M_n = 9400 \text{ g}\cdot\text{mol}^{-1}$, $M_w = 19,400 \text{ g}\cdot\text{mol}^{-1}$, PDI = 2.0 and $D_p = 10$; chloroform fraction, $M_n = 20,000 \text{ g}\cdot\text{mol}^{-1}$, $M_w = 44,900 \text{ g}\cdot\text{mol}^{-1}$, PDI = 2.2 and $D_p = 22$. ^1H NMR (toluene fraction) ($\text{C}_2\text{D}_2\text{Cl}_4$, δ): 8.02 (d, 2H, $J = 3.5 \text{ Hz}$), 7.96 (s, 2H), 7.87 (d, 2H, $J = 11.0 \text{ Hz}$), 7.80 (d, 2H, $J = 8.0 \text{ Hz}$), 7.50 (d, 2H, $J = 3.0 \text{ Hz}$), 3.90–3.68 (bm, 2H), 1.89–1.67 (bm, 1H), 1.62–1.29 (bm, 9H), 1.28–1.12 (bm, 24H), 1.12–1.03 (bm, 4H), 1.03–0.95 (bm, 3H), 0.86 (d, 6H, $J = 6.5 \text{ Hz}$), 0.84–0.79 (bm, 6H). FT-IR (cm^{-1}): 2953, 2918, 2850, 1754, 1698, 1556, 1432, 1364, 1254, 1173, 1063. EA (%) calculated for $\text{C}_{54}\text{H}_{65}\text{N}_3\text{O}_2\text{S}_3\text{Si}$: C, 71.09; H, 7.18; N, 4.61; S, 10.54. Found: C, 69.43; H, 7.00; N, 4.36; S, 10.08.

2.3.24. Synthesis of poly[9,9-dioctyl-2,7-dibenzosilole-alt-5,5-(4',7'-bis(2-thienyl)-2',1',3'-benzothiadiazole-5,6-N-octyl-dic arboxylicimide)] (PDBSDBTBTDI-8)

PDBSDBTBTDI-8 was prepared followed by the same procedure for synthesis of PFDTBTBTDI-DMO. M4 (147.5 mg, 0.224 mmol) and M2 (143.2 mg, 0.224 mmol) were copolymerized for 22 h to afford PDBSDBTBTDI-8 as purple powders. Toluene fraction (66 mg, 0.07 mmol, 33% yield), chloroform fraction (52 mg, 0.05 mmol, 26% yield) with total yield 59% [21]. GPC: toluene fraction, $M_n = 10,000 \text{ g}\cdot\text{mol}^{-1}$, $M_w = 26,200 \text{ g}\cdot\text{mol}^{-1}$, PDI = 2.6 and $D_p = 11$; chloroform fraction, $M_n = 16,100 \text{ g}\cdot\text{mol}^{-1}$, $M_w = 38,700 \text{ g}\cdot\text{mol}^{-1}$, PDI = 2.4 and $D_p = 18$. ^1H NMR (toluene fraction) ($\text{C}_2\text{D}_2\text{Cl}_4$, δ): 8.02 (d, 2H, $J = 3.5 \text{ Hz}$), 7.96 (s, 2H), 7.87 (d, 2H, $J = 11.0 \text{ Hz}$), 7.80 (d, 2H, $J = 8.0 \text{ Hz}$), 7.50 (d, 2H, $J = 3.0 \text{ Hz}$), 3.90–3.68 (bm, 2H), 1.81–1.69 (bm, 2H), 1.53–1.15 (bm, 34H), 1.12–1.03 (bm, 4H), 0.88 (t, 3H, $J = 6.5 \text{ Hz}$), 0.85–0.80 (bm, 6H). FT-IR (cm^{-1}): 2950, 2921, 2854, 1758, 1701, 1556, 1428, 1364, 1254, 1166, 1003. EA (%) calculated for $\text{C}_{52}\text{H}_{61}\text{N}_3\text{O}_2\text{S}_3\text{Si}$: C, 70.63; H, 6.95; N, 4.75; S, 10.88. Found: C, 69.92; H, 6.85; N, 4.60; S, 10.22.

3. Results and Discussions

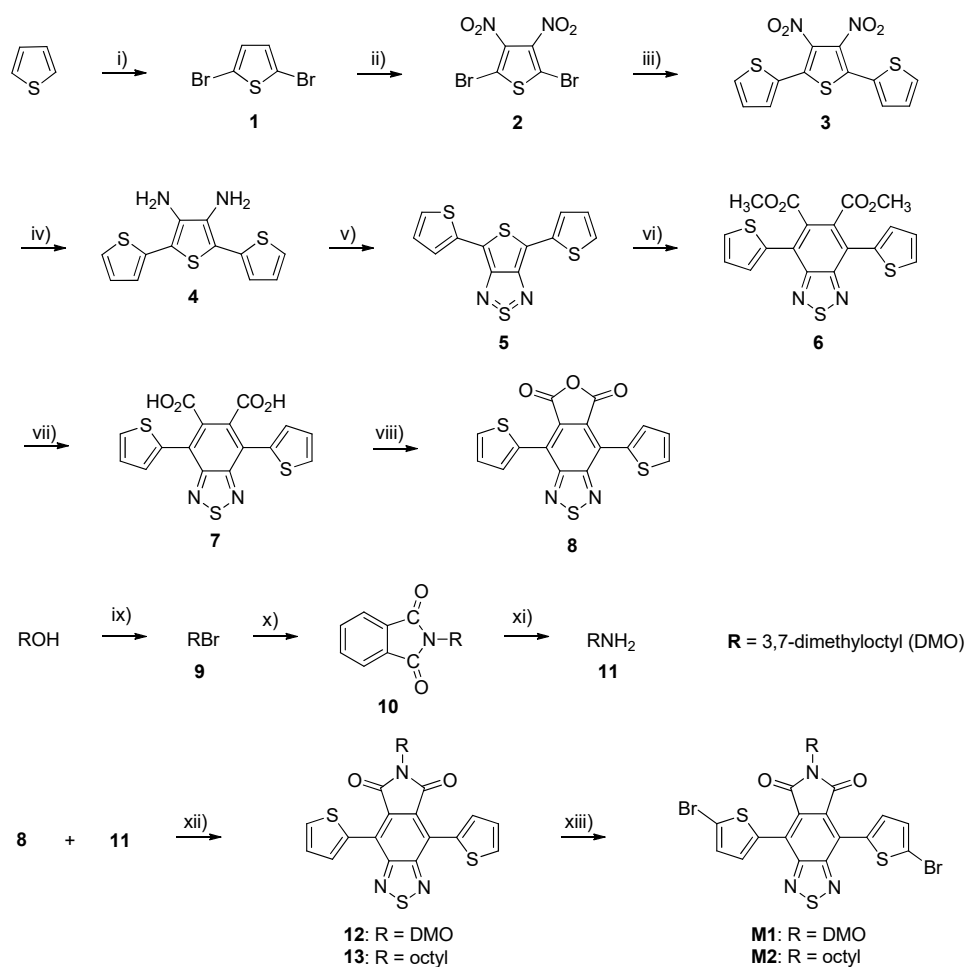
3.1. Synthesis of Monomers and Polymers

The synthetic methods for the preparation of benzothiadiazole dicarboxylic imide (BTDI) monomers (M1 and M2) are outlined in Scheme 1. M1 and M2 were synthesized through several steps starting from commercially available thiophene. For the synthesis of 2,5-dibromothiophene (1), thiophene was selectively brominated at 2,5-positions using two equivalents of *N*-bromosuccinimide (NBS) in DMF in the dark to give 1 as a yellow oily product in a high yield [37]. Then 1 was nitrated with concentrated nitric acid/sulfuric acid and fuming sulfuric acid to give 2,5-dibromo-3,4-dinitrothiophene (2) [38,51,52]. The compound 2 was then reacted with 2-(tributylstannyl) thiophene in the presence of $\text{PdCl}_2(\text{PPh}_3)_2$ as a catalyst in anhydrous toluene at $115 \text{ }^\circ\text{C}$ to give 3',4'-dinitro-2,2':5',2''-terthiophene (3). The resulting compound was obtained as orange crystals in an excellent yield of 90% [39]. 3',4'-diamino-2,2':5',2''-terthiophene (4) was obtained by a reduction reaction of 3 using excess anhydrous tin (II) chloride (SnCl_2). 4 was achieved as a brown solid in an excellent yield of 97% [40]. The resulting substance (4) was then reacted with *N*-thionyl aniline (PhNSO) and trimethylsilyl chloride (TMSCl) in anhydrous pyridine to afford 4,6-bis(2-thienyl)-thieno[3,4-*c*][1,2,5]-thiadiazole (5) as blue crystals in an excellent yield of 93% [41]. The compound 4,7-di(thien-2-yl)-2,1,3-benzothiadiazole-5,6-dimethyl ester (6) was obtained by the Diels-Alder reaction between 5 and dimethyl acetylenedicarboxylate in anhydrous xylene at reflux. It was obtained in an excellent yield of 94% as yellow crystals [23]. Next, the material 6 was hydrolyzed under basic conditions in ethanol under reflux followed by acidification to yield 4,7-di(thien-2-yl)-2,1,3-benzothiadiazole-5,6-dicarboxylic acid (7) as a yellow solid in a yield of 85% [20].

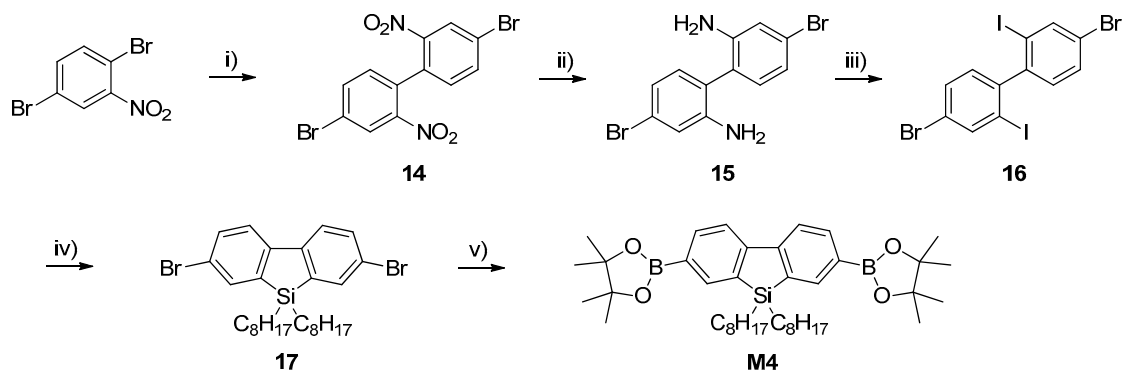
The compound 4,7-di(thien-2-yl)-2,1,3-benzothiadiazole-5,6-dicarboxylic anhydride (8) was synthesized by intramolecular ring closure of 7, in the presence of acetic anhydride and anhydrous xylene at 130 °C, to afford 8 as a red solid in an excellent yield of 97% [42]. 3,7-dimethyloctyl bromide (9) was synthesized from the reaction of commercially available 3,7-dimethyl-1-octanol with triphenylphosphine (Ph₃P)/NBS in dichloromethane to yield 9 as a colorless oil in 73% yield [43]. Then, 9 was reacted with potassium phthalimide in anhydrous DMF to give *N*-(3,7-dimethyloctyl)phthalimide (10) as colorless oil in an excellent yield of 91% [44]. 3,7-dimethyl-1-octanamine (11) was obtained by Gabriel synthesis from the reaction of 10 with hydrazine hydrate (NH₂NH₂) in methanol as brown oil in 86% yield [45]. The compounds 4,7-di(thien-2-yl)-2,1,3-benzothiadiazole-5,6-*N*-(3,7-dimethyloctyl)dicarboxylic imide (12) and 4,7-di(thien-2-yl)-2,1,3-benzothiadiazole-5,6-*N*-octyl-dicarboxylic imide (13) were synthesized by the reaction of 8 with 11 and 1-octanamine in the presence of acetic acid and acetic anhydride to yield imide functionalized monomers (12 and 13) as orange solids in 84 and 93% yield, respectively [42]. Lastly, the monomers 4,7-di(5-bromo-thien-2-yl)-2,1,3-benzothiadiazole-5,6-*N*-(3,7-dimethyloctyl)dicarboxylic imide (M1) and 4,7-di(5-bromo-thien-2-yl)-2,1,3-benzothiadiazole-5,6-*N*-octyl-dicarboxylic imide (M2) were prepared by the bromination of 12 and 13 at 5,5'-positions using NBS in THF and to yield M1 and M2 as red solids in excellent yields of 98 and 96%, respectively [20].

Reagents and conditions: (i) NBS, DMF, -15 °C, RT, overnight; (ii) fuming H₂SO₄ (20% free SO₃), conc. H₂SO₄, conc. HNO₃, 20 °C, 20–30 °C, 3 h; (iii) 2-(tributylstannyl) thiophene, anhydrous toluene, PdCl₂(PPh₃)₂, 115 °C, 24 h; (iv) anhydrous SnCl₂, HCl (35%), ethanol, 30 °C, 24 h, NaOH (25%); (v) PhNSO, TMSCl, anhydrous pyridine, 3 hours, RT, HCl (1.0 N); (vi) dimethyl acetylenedicarboxylate, anhydrous xylene, reflux 24 h; (vii) aqueous NaOH, ethanol, reflux 24 h, HCl (35%); (viii) anhydrous Ac₂O, anhydrous xylene, 130 °C, 6 h; (ix) DCM, PPh₃, NBS, RT, 90 min; (x) potassium phthalimide, anhydrous DMF, 90 °C, 17 h, KOH; (xi) hydrazine hydrate (51%), methanol, reflux, HCl (5.0 M), reflux, 1 h; (xii) HOAc (100%), 100 °C overnight, Ac₂O, 100 °C, 6 h; (xiii) NBS, THF, RT, overnight.

The diboronic ester of dibenzosilole (DBS) monomer (M4) was synthesized through five steps starting from the commercially available 2,5-dibromonitrobenzene. The steps in its preparation is outlined in Scheme 2. The first step was the synthesis of 4,4'-dibromo-2,2'-dinitrobiphenyl (14) by the Ullmann coupling reaction using 2,5-dibromonitrobenzene and copper powder in anhydrous DMF and the resulting material was yellow crystals and gave an excellent yield of 90% [46]. Then, 14 was reduced using tin metal in ethanol under acidic medium to obtain 4,4'-dibromobiphenyl-2,2'-diamine (15) as brown crystals in a yield of 70% [47]. Next, 4,4'-dibromo-2,2'-diiodobiphenyl (16) was prepared by the reaction of 15 with a mixture of aqueous sodium nitrite and HCl in acetonitrile which was subsequently treated with aqueous potassium iodide to give 16 *via* the Sandmeyer type reaction as white crystals in a yield of 51% [48]. Then, 16 was reacted with *n*-BuLi in anhydrous THF and subsequently treated with dichlorodioctylsilane [(C₈H₁₇)₂SiCl₂] to obtain 2,7-dibromo-9,9-dioctyldibenzosilole (17) as colorless oil in 90% yield [49]. Finally, 9,9-dioctyl-2,7-bis(4,4,5,5-tetramethyl-1,3,2-dioxaborolan-2-yl)-dibenzosilole (M4) was synthesized by the reaction of 17 with an excess of bis(pinacolato)diboron/potassium acetate base and PdCl₂(dppf) catalyst in anhydrous DMF which yielded M4 as brown crystals in 53% yield (Scheme 2) [50].



Scheme 1. Synthetic steps of the 4,7-di(5-bromo-thien-2-yl)-2,1,3-benzothiadiazole-5,6-N-(3,7-dimethyloctyl)dicarboxylic imide (M1) and 4,7-di(5-bromo-thien-2-yl)-2,1,3-benzothiadiazole-5,6-N-octyl-dicarboxylic imide (M2).

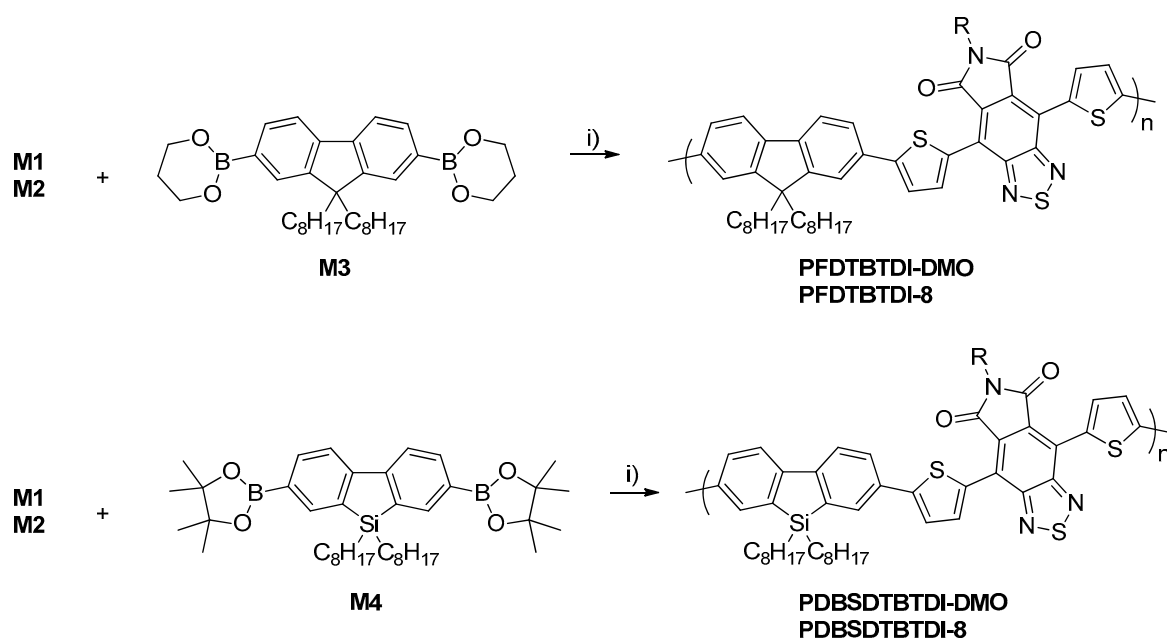


Scheme 2. Synthetic steps of the monomer 9,9-dioctyl-2,7-bis(4,4,5,5-tetramethyl-1,3,2-dioxaborolan-2-yl)-dibenzosilole (M4).

Reagents and conditions: (i) Cu, DMF, 125 °C, 3 h; (ii) Sn, HCl (32%), ethanol, 3 h, reflux, NaOH (20%); (iii) HCl (32%), acetonitrile, NaNO₂, 0 °C, −5 to −10 °C, KI, 0 °C, −10 to −15 °C, RT, 80 °C, 20 h, Na₂S₂O₃; (iv) anhydrous THF, −78 °C, *n*-BuLi, 3 h, dichlorodioctylsilane, RT, overnight; (v) bis(pinacolato)diboron, PdCl₂(dppf), KOAc, anhydrous DMF, 100 °C, 48 h.

In this article, the synthesis of four alternating D-A copolymers, PFDTBTDI-DMO, PFDTBTDI-8, PDBSDTBTDI-DMO, and PDBSDTBTDI-8 is described in Scheme 3. The polymers were prepared by

the Suzuki polymerization between bis-boronate esters (M3 and M4) with dibromides (M1 and M2), respectively. The polymerizations were performed using Pd(OAc)₂/P(*o*-tol)₃ catalyst, NaHCO₃ base in anhydrous THF. All polymerizations were left for 21–30 h with large amounts of purple precipitates forming as the reactions proceeded. The structures of the PFDTBTDI-DMO, PFDTBTDI-8, PDBSDBTDI-DMO, and PDBSDBTDI-8 were verified by the ¹H NMR spectroscopy, FT-IR spectroscopy and elemental analysis. The ¹H NMR spectra for the polymers are available in Supplementary Information.



Scheme 3. (i) The synthesis of poly[9,9-dioctyl-2,7-fluorene-alt-5,5-(4',7'-bis(2-thienyl)-2',1',3'-benzothiadiazole-5,6-N-(3,7-dimethyloctyl)dicarboxylic imide)] (PFDTBTDI-DMO), poly[9,9-dioctyl-2,7-fluorene-alt-5,5-(4',7'-bis(2-thienyl)-2',1',3'-benzothiadiazole-5,6-N-octyl-dicarboxylic imide)] (PFDTBTDI-8), poly[9,9-dioctyl-2,7-dibenzosilole-alt-5,5-(4',7'-bis(2-thienyl)-2',1',3'-benzothiadiazole-5,6-N-(3,7-dimethyloctyl)dicarboxylic imide)] (PDBSDBTDI-DMO) and (ii) poly[9,9-dioctyl-2,7-dibenzosilole-alt-5,5-(4',7'-bis(2-thienyl)-2',1',3'-benzothiadiazole-5,6-N-octyl-dicarboxylic imide)] (PDBSDBTDI-8) via Suzuki polymerization.

Reagents and conditions: (i) anhydrous THF, NaHCO₃, Pd(OAc)₂, P(*o*-tol)₃, 90 °C, 21–30 h.

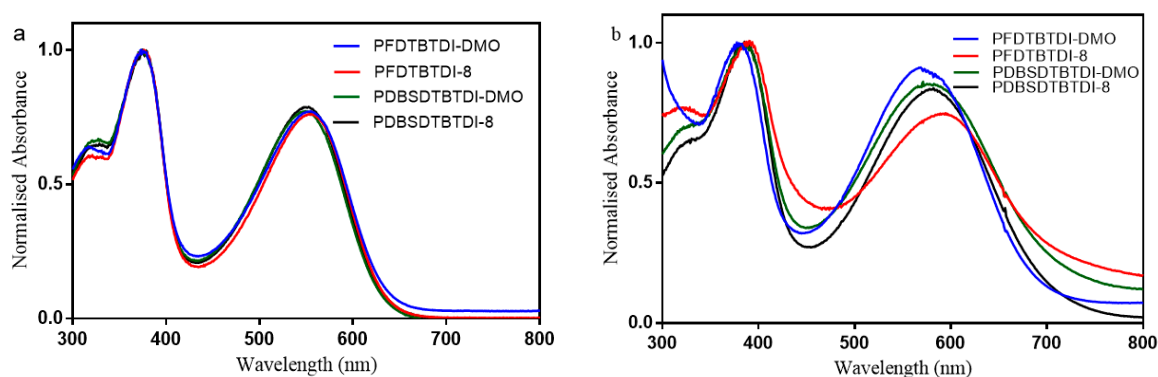
Molecular weights of the polymers were measured by GPC using chloroform at 40 °C relative to polystyrene standards, as shown in Table 1. Substituting 3,7-dimethyloctyl chains in PFDTBTDI-DMO for octyl chains in PFDTBTDI-8 on the BTDI building blocks results in a polymer with lower M_n values for the toluene fractions of the polymers. However, PFDTBTDI-8 afforded another fraction in chloroform of a higher M_n value that was not soluble in toluene while PFDTBTDI-DMO did not provide chloroform fraction. The results indicate that a higher solubility of the polymer with 3,7-dimethyloctyl chains as a result of the branching of its substituents. The toluene fractions of the dibenzosilole-based polymers (PDBSDBTDI-DMO and PDBSDBTDI-8) have similar M_n values. However, PDBSDBTDI-8 has a lower M_n value to that of PDBSDBTDI-DMO for the chloroform fractions. This could be attributed to the effect of the branched chains in PDBSDBTDI-DMO which provides it with a greater solubility and allows it to provide higher molecular weight fractions. Polymers with *n*-octyl chains provided lower yields compared to those with branched chains. Moreover, the yield of fluorene-based polymers is higher relative to dibenzosilole-based polymers. This could be due to more aggregation in dibenzosilole-based polymers with more intermolecular interactions relative to fluorene-based polymers.

Table 1. The percentage yield, weight and number average molecular weights with polydispersity indexes of PFDTBTDI-DMO, PFDTBTDI-8, PDBSDTBTDI-DMO, and PDBSDTBTDI-8.

Polymer	Toluene Fraction			Chloroform Fraction		
	M_n (g·mol ⁻¹)	M_w (g·mol ⁻¹)	PDI	M_n (g·mol ⁻¹)	M_w (g·mol ⁻¹)	PDI
PFDTBTDI-DMO	16,000	33,000	2.0	-	-	-
PFDTBTDI-8	11,200	29,100	2.5	24,900	74,400	2.9
PDBSDTBTDI-DMO	9400	19,400	2.0	20,000	44,900	2.2
PDBSDTBTDI-8	10,000	26,200	2.6	16,100	38,700	2.4

3.2. Optical Properties

The normalized UV-vis absorption spectra of all polymers in chloroform solutions and in thin films are shown in Figure 1. The optical properties of these polymers are summarized in Table 2. All polymers show two absorption bands at short and long wavelengths. The peak at shorter wavelengths could be related to π - π^* transition. However, the other band at lower energy is related to the intramolecular charge transfer (ICT) between donor (D) and acceptor (A) units. The band gaps (E_g) of the polymers are assessed from the absorption onsets in thin films. In solutions, all polymers display comparable absorption maxima. In thin films, the absorption spectra of the polymers show red-shifted absorption maxima by 22–34 nm relative to their absorption in solutions. This could be explained by stronger intermolecular π - π interaction and a more planar structure in the solid state. Compared with fluorene-based polymers, dibenzosilole-based polymers have broader absorption bands and therefore lower E_g values. A change of alkyl chains on BTDI units from 3,7-dimethyloctyl chains to *n*-octyl chains has a negligible impact on the E_g of the resulting polymers. PFDTBTDI-8 is red-shifted relative to its PFDTBTDI-DMO analogue; this may arise from the fact that the former polymer has a higher molecular weight than the latter polymer.

**Figure 1.** Normalized UV-vis absorption spectra of PFDTBTDI-DMO, PFDTBTDI-8, PDBSDTBTDI-DMO, and PDBSDTBTDI-8 in (a) chloroform solutions; and (b) thin films.**Table 2.** The UV-vis data and optical band gaps of the polymers.

Polymer	ϵ (M ⁻¹ ·cm ⁻¹)	Solution		Film	
		λ_{max} (nm)	λ_{max} (nm)	λ_{onset} (nm)	E_g (eV)
PFDTBTDI-DMO	26,200	550	572	685	1.81
PFDTBTDI-8	22,900	551	585	696	1.78
PDBSDTBTDI-DMO	35,500	550	576	700	1.77
PDBSDTBTDI-8	34,900	550	578	697	1.77

PFDTBTDI-DMO and PFDTBTDI-8 have lower E_g relative to P(BTI-F) which has two extra thiophene spacers between fluorene and DTBTDI units. The latter polymer is blue-shifted around

10–25 nm relative to the former polymers. PFDTBTDI-DMO and PFDTBTDI-8 have lower E_g values around 0.1 eV compared with that of PFDTBT due to the stronger electron-accepting strength of the BTDI building blocks than BT unit [18]. Similarly, PDBSDBTBTDI-DMO and PDBSDBTBTDI-8 have lower E_g relative to PDBSDBTBT analogue [35]. The absorption coefficients (ϵ) of the dibenzosilole-based polymers are higher than fluorene-based polymers as illustrated in Table 2. This indicates that all things been equal, the dibenzosilole polymers should lead to more efficient OPV devices.

3.3. Electrochemical Properties

Cyclic voltammetry (CV) is considered to be an effective technique to study the electroactivity of active species and it is also suitable technique for characterizing the oxidation and reduction potentials of the different phases present in the conducting polymers [53]. In addition, CV can be employed to analyze the charge storage mechanism and the charge transfer between the electrodes in the electrochemical double layer capacitor (EDLC) [54–56]. Therefore, in this work CV was used to study the electrochemical properties of the polymers. The LUMO and HOMO levels of all polymers calculated from the onsets of reduction and oxidation potentials, respectively (Figure 2 and Table 3). The onsets were determined from cyclic voltammograms on drop cast polymer films on Pt electrode as working electrode in $\text{Bu}_4\text{NClO}_4/\text{CH}_3\text{CN}$ (0.1 M) vs. Ag/Ag^+ reference electrode. All polymers show the same HOMO energy levels. The results indicate that switching from fluorene to DBS moiety does not alter the HOMO levels of the resulting polymers. The HOMO level is dominated by the nature of the donor unit and that both fluorene and DBS units are weak electron donors of comparable strength. All polymers display low-lying HOMO energy levels which are beneficial for the chemical stability of polymers in oxygen and should lead to higher V_{oc} values of the fabricated OPV devices including these polymers as donor materials. All polymers have nearly identical LUMO energy levels, as all polymers have the same BTDI acceptor units which control the LUMO levels in these materials. Furthermore, anchoring different alkyl chains on BTDI units has little impact on the LUMO levels of the resulting polymers.

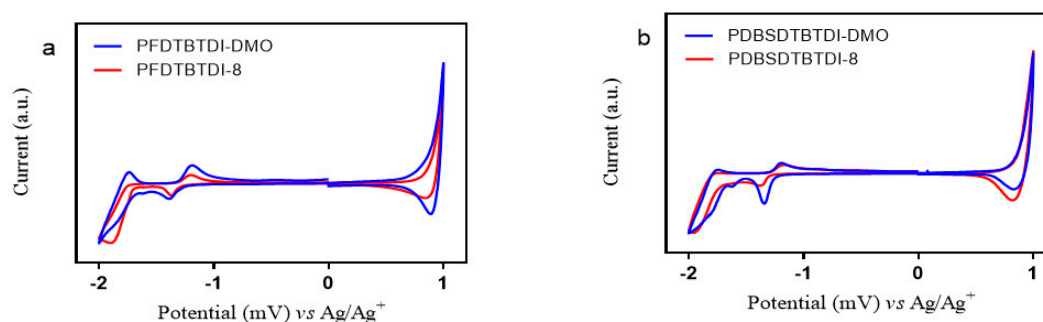


Figure 2. Cyclic voltammograms of (a) PFDTBTDI-DMO and PFDTBTDI-8; (b) PDBSDBTBTDI-DMO and PDBSDBTBTDI-8 on Pt electrode in $\text{Bu}_4\text{NClO}_4/\text{CH}_3\text{CN}$ at 100 mV/s.

Table 3. Thermal and electrochemical properties of the polymers.

Polymer	T_d (°C)	E_{ox}^0 (V)	HOMO (eV)	E_{red}^0 (V)	LUMO (eV)	$E_g^{(elec)}$ (eV)
PFDTBTDI-DMO	409	0.87	−5.59	1.27	−3.44	2.15
PFDTBTDI-8	367	0.87	−5.59	1.27	−3.44	2.15
PDBSDBTBTDI-DMO	438	0.87	−5.59	1.25	−3.46	2.12
PDBSDBTBTDI-8	359	0.87	−5.59	1.29	−3.42	2.16

All polymers have comparable HOMO levels relative to P(BTI-F), which has a HOMO level of −5.60 eV [24]. This indicates that the incorporation of two extra thiophene spacers between fluorene and DTBTDI units has negligible effect on the HOMO levels of the resulting polymers.

However, all polymers have deeper HOMO levels compared to those of PDI-BDIT, PDI-BDIO, BBTI-1, and BBTI-2. This could be attributed to fluorene and DBS units being weaker electron donors than BDT and BTT units [20,23]. The LUMO levels of the polymers are higher than those of PFDTBT and PDBSDTBT (−3.8 eV), which are related to the stronger electron-accepting ability of BTDI moiety than BT unit [18,35].

3.4. Thermal Properties

The thermal properties of the polymers were studied by TGA (Figure 3 and Table 3). All polymers show high thermal stability with T_d up to 350 °C. The thermal stability of the polymers with *n*-octyl chains on BTDI moiety is significantly lower than those with 3,7-dimethyloctyl chains. The results show that the thermal properties of the polymers are mostly affected by the size of the alkyl chains anchored to the BTDI units as well as by the type of the donor building blocks.

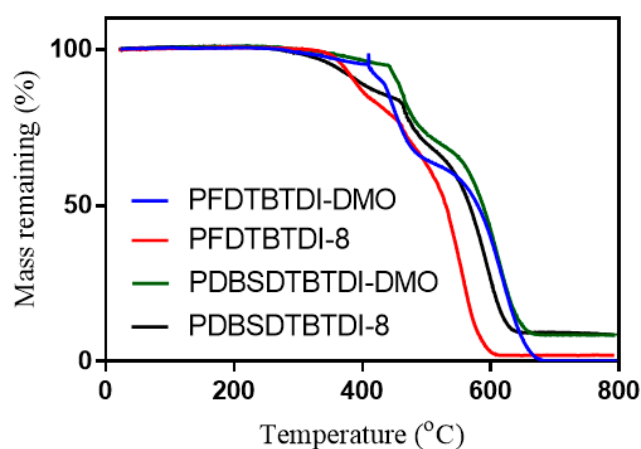


Figure 3. TGA of PFDTBTDI-DMO, PFDTBTDI-8, PDBSDTBTDI-DMO, and PDBSDTBTDI-8.

3.5. Powder X-ray Diffraction (XRD)

Since a single polymer can come in various forms including crystalline, amorphous and semi-crystalline phases, which effect on its mechanical and electrical properties, it is necessary to accurately determine the structural properties using XRD technique [57–59]. The structural properties of the prepared polymers were investigated by powder XRD in solid state as shown in Figure 4. The XRD of the PFDTBTDI-DMO, PFDTBTDI-8, PDBSDTBTDI-DMO, and PDBSDTBTDI-8 show diffraction peaks at 20.0°, 20.5°, 19.7° and 20.3° corresponding to the π - π stacking distance of 4.43 Å, 4.32 Å, 4.5 Å and 4.36 Å, respectively. The results presented in the current study confirm that all the prepared polymers have an amorphous nature, which are similar to the most conductive polymers from the literature [53,60,61]. It is also worth noting that the peaks for the polymers containing *n*-octyl chains are more pronounced which indicates more aggregation than those polymers including 3,7-dimethyloctyl chains as also indicated by their lower solubility.

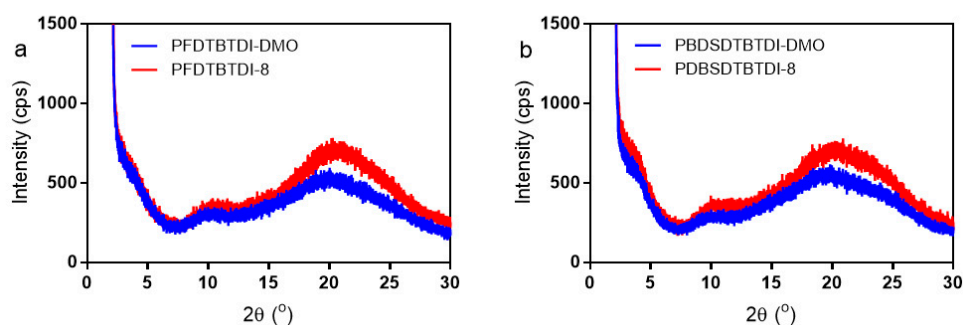


Figure 4. Powder XRD of (a) PFDTBTDI-DMO and PFDTBTDI-8; (b) PDBSDBTBTDI-DMO and PDBSDBTBTDI-8.

4. Conclusions

In summary, four fluorene and dibenzosilole-based copolymers were prepared by copolymerizing 2,7-fluorene and 2,7-dibenzosilole (DBS) with both M1 and M2 and yielded PFDTBTDI-DMO, PFDTBTDI-8, PDBSDBTBTDI-DMO, and PDBSDBTBTDI-8, respectively. All polymers exhibit good solubility in common organic solvents. Changing the alkyl chains on BTDI moieties has a substantial influence on the solubility of the polymers. The use of 3,7-dimethyloctyl side groups on BTDI units in the fluorene-based polymers afforded PFDTBTDI-DMO in high yield; however, the polymer was extracted in the toluene fraction due to its high solubility. The use of *n*-octyl side groups on BTDI units yielded PFDTBTDI-8, which has a lower solubility. In addition to the toluene fraction, another fraction from chloroform which a higher molecular weight was obtained. However, in the case of dibenzosilole-based copolymers, linear octyl side chains have a negative impact on the molecular weight and the solubility of the resulting polymer. In solutions, all polymers show similar absorption maxima. In thin films, the absorption spectra of the polymers display bathochromic shift absorption maxima relative to their absorption in solutions. The optical band gaps of the fluorene-based copolymers are slightly higher than those of dibenzosilole-based copolymers. The band gaps of the fluorene-based polymers are slightly changed by substituting 3,7-dimethyloctyl chains with *n*-octyl chains on BTDI units, while the band gaps of dibenzosilole-based polymers are the same. Upon varying fluorene to DBS unit, the HOMO levels of the resulting polymers do not change. This is due to the fact that the HOMO energy levels are controlled by the nature of the donor units, both fluorine and DBS units are weak electron donors of similar strength. All polymers show deep-lying HOMO energy levels of -5.59 eV, which are advantageous for the chemical stability, and this would lead to higher V_{oc} values using these polymers as electron-donating materials in the BHJ devices. All polymers have almost the same LUMO levels since they have the same BTDI acceptor units which dominate the LUMO levels in these materials. Moreover, attaching different alkyl chains on BTDI units has little impact on the LUMO energy levels of the resulting polymers. All polymers show excellent thermal stability with T_d exceeding 350 °C. The polymers based on branched 3,7-dimethyloctyl chains have higher thermal stability than those polymers based on *n*-octyl chains. The thermal stability of the polymers is dependent upon the type of the alkyl substituents attached to the acceptor moieties. The X-ray powder diffraction studies of the polymers show diffraction peaks around 20.0° corresponding to the π - π stacking distance of about 4.0 Å which gives evidence for the amorphous nature of the polymer. All polymers have the amorphous nature.

Supplementary Materials: The following are available online at <http://www.mdpi.com/2079-6412/10/12/1147/s1>, Figure S1: ^1H NMR spectrum of PFDTBTDI-DMO in $\text{C}_2\text{D}_2\text{Cl}_4$ at 100 °C. Figure S2: ^1H NMR spectrum of PFDTBTDI-8 in $\text{C}_2\text{D}_2\text{Cl}_4$ at 100 °C. Figure S3: ^1H NMR spectrum of PDBSDBTBTDI-DMO in $\text{C}_2\text{D}_2\text{Cl}_4$ at 100 °C. Figure S4: ^1H NMR spectrum of PDBSDBTBTDI-8 in $\text{C}_2\text{D}_2\text{Cl}_4$ at 100 °C.

Author Contributions: Conceptualization, A.I. and S.B.A.; Formal analysis, A.R.M.; Investigation, A.R.M.; Project administration, A.R.M., A.R. and S.B.A.; Supervision, A.I.; Validation, A.I., S.B.A., S.N.A., R.T.A. and S.A.H.;

Writing—original draft, A.R.M.; Writing—review & editing, A.I., S.B.A., S.N.A., R.T.A. and S.A.H. All authors have read and agreed to the published version of the manuscript.

Funding: This research received no external funding.

Conflicts of Interest: The authors declare no conflict of interest.

References

1. Günes, S.; Neugebauer, H.; Sariciftci, N.S. Conjugated polymer-based organic solar cells. *Chem. Rev.* **2007**, *107*, 1324–1338. [[CrossRef](#)] [[PubMed](#)]
2. Thompson, B.C.; Frechet, J.M. Polymer–fullerene composite solar cells. *Angew. Chem. Int. Ed.* **2008**, *47*, 58–77. [[CrossRef](#)] [[PubMed](#)]
3. Cheng, Y.-J.; Yang, S.-H.; Hsu, C.-S. Synthesis of conjugated polymers for organic solar cell applications. *Chem. Rev.* **2009**, *109*, 5868–5923. [[CrossRef](#)]
4. Duan, C.; Huang, F.; Cao, Y. Recent development of push–pull conjugated polymers for bulk-heterojunction photovoltaics: Rational design and fine tailoring of molecular structures. *J. Mater. Chem.* **2012**, *22*, 10416–10434. [[CrossRef](#)]
5. Yu, G.; Gao, J.; Hummelen, J.C.; Wudl, F.; Heeger, A.J. Polymer photovoltaic cells: Enhanced efficiencies via a network of internal donor–acceptor heterojunctions. *Science* **1995**, *270*, 1789. [[CrossRef](#)]
6. Yu, G.; Heeger, A.J. Charge separation and photovoltaic conversion in polymer composites with internal donor/acceptor heterojunctions. *J. Appl. Phys.* **1995**, *78*, 4510–4515. [[CrossRef](#)]
7. Li, Y. Molecular design of photovoltaic materials for polymer solar cells: Toward suitable electronic energy levels and broad absorption. *Acc. Chem. Res.* **2012**, *45*, 723–733. [[CrossRef](#)] [[PubMed](#)]
8. Zhang, Z.G.; Wang, J. Structures and properties of conjugated Donor–Acceptor copolymers for solar cell applications. *J. Mater. Chem.* **2012**, *22*, 4178–4187. [[CrossRef](#)]
9. Kim, H.I.; Kim, M.J.; Choi, K.; Lim, C.; Kim, Y.H.; Kwon, S.K.; Park, T. Improving the Performance and Stability of Inverted Planar Flexible Perovskite Solar Cells Employing a Novel NDI-Based Polymer as the Electron Transport Layer. *Adv. Energy Mater.* **2018**, *8*, 1702872. [[CrossRef](#)]
10. Chen, J.; Cao, Y. Development of novel conjugated donor polymers for high-efficiency bulk-heterojunction photovoltaic devices. *Acc. Chem. Res.* **2009**, *42*, 1709–1718. [[CrossRef](#)]
11. Hou, J.; Chen, H.-Y.; Zhang, S.; Li, G.; Yang, Y. Synthesis, characterization, and photovoltaic properties of a low band gap polymer based on silole-containing polythiophenes and 2, 1, 3-benzothiadiazole. *J. Am. Chem. Soc.* **2008**, *130*, 16144–16145. [[CrossRef](#)] [[PubMed](#)]
12. Zhu, Z.; Waller, D.; Gaudiana, R.; Morana, M.; Mühlbacher, D.; Scharber, M.; Brabec, C. Panchromatic conjugated polymers containing alternating donor/acceptor units for photovoltaic applications. *Macromolecules* **2007**, *40*, 1981–1986. [[CrossRef](#)]
13. Huo, L.; Chen, H.-Y.; Hou, J.; Chen, T.L.; Yang, Y. Low band gap dithieno [3, 2-b: 2', 3'-d] silole-containing polymers, synthesis, characterization and photovoltaic application. *Chem. Commun.* **2009**, *37*, 5570–5572. [[CrossRef](#)] [[PubMed](#)]
14. Chen, M.H.; Hou, J.; Hong, Z.; Yang, G.; Sista, S.; Chen, L.M.; Yang, Y. Efficient polymer solar cells with thin active layers based on alternating polyfluorene copolymer/fullerene bulk heterojunctions. *Adv. Mater.* **2009**, *21*, 4238–4242. [[CrossRef](#)]
15. Slooff, L.; Veenstra, S.; Kroon, J.; Moet, D.; Sweelssen, J.; Koetse, M. Determining the internal quantum efficiency of highly efficient polymer solar cells through optical modeling. *Appl. Phys. Lett.* **2007**, *90*, 143506. [[CrossRef](#)]
16. Boudreault, P.-L.T.; Najari, A.; Leclerc, M. Processable low-bandgap polymers for photovoltaic applications. *Chem. Mater.* **2010**, *23*, 456–469. [[CrossRef](#)]
17. Zhou, H.; Yang, L.; You, W. Rational design of high performance conjugated polymers for organic solar cells. *Macromolecules* **2012**, *45*, 607–632. [[CrossRef](#)]
18. Svensson, M.; Zhang, F.; Inganäs, O.; Andersson, M. Synthesis and properties of alternating polyfluorene copolymers with redshifted absorption for use in solar cells. *Synth. Met.* **2003**, *135*, 137–138. [[CrossRef](#)]
19. Zhou, P.; Zhang, Z.-G.; Li, Y.; Chen, X.; Qin, J. Thiophene-Fused Benzothiadiazole: A Strong Electron-Acceptor Unit to Build D–A Copolymer for Highly Efficient Polymer Solar Cells. *Chem. Mater.* **2014**, *26*, 3495–3501. [[CrossRef](#)]

20. Nielsen, C.B.; Ashraf, R.S.; Treat, N.D.; Schroeder, B.C.; Donaghey, J.E.; White, A.J.; Stingelin, N.; McCulloch, I. 2, 1, 3-Benzothiadiazole-5, 6-Dicarboxylic Imide—A Versatile Building Block for Additive-and Annealing-Free Processing of Organic Solar Cells with Efficiencies Exceeding 8%. *Adv. Mater.* **2015**, *27*, 948–953. [[CrossRef](#)]
21. Yi, H.; Al-Faifi, S.; Iraqi, A.; Watters, D.C.; Kingsley, J.; Lidzey, D.G. Carbazole and thienyl benzo [1, 2, 5] thiadiazole based polymers with improved open circuit voltages and processability for application in solar cells. *J. Mater. Chem.* **2011**, *21*, 13649–13656. [[CrossRef](#)]
22. Zhou, H.; Yang, L.; Stuart, A.C.; Price, S.C.; Liu, S.; You, W. Development of fluorinated benzothiadiazole as a structural unit for a polymer solar cell of 7% efficiency. *Angew. Chem.* **2011**, *123*, 3051–3054. [[CrossRef](#)]
23. Wang, L.; Cai, D.; Zheng, Q.; Tang, C.; Chen, S.-C.; Yin, Z. Low Band Gap Polymers Incorporating a Dicarboxylic Imide-Derived Acceptor Moiety for Efficient Polymer Solar Cells. *ACS Macro Lett.* **2013**, *2*, 605–608. [[CrossRef](#)]
24. Li, H. A high voltage solar cell using a donor–acceptorconjugated polymer based on pyrrolo[3,4-f]-2,1,3-benzothiadiazole-5,7-dione. *J. Mater. Chem.* **2014**, *2*, 17925–17933. [[CrossRef](#)]
25. Gadisa, A.; Mammo, W.; Andersson, L.M.; Admassie, S.; Zhang, F.; Andersson, M.R.; Inganäs, O. A new donor–acceptor–donor polyfluorene copolymer with balanced electron and hole mobility. *Adv. Funct. Mater.* **2007**, *17*, 3836–3842. [[CrossRef](#)]
26. Zhang, F.; Mammo, W.; Andersson, L.M.; Admassie, S.; Andersson, M.R.; Inganäs, O. Low-bandgap alternating fluorene copolymer/methanofullerene heterojunctions in efficient near-infrared polymer solar cells. *Adv. Mater.* **2006**, *18*, 2169–2173. [[CrossRef](#)]
27. Zhang, F.; Bijleveld, J.; Perzon, E.; Tvingstedt, K.; Barrau, S.; Inganäs, O.; Andersson, M.R. High photovoltage achieved in low band gap polymer solar cells by adjusting energy levels of a polymer with the LUMOs of fullerene derivatives. *J. Mater. Chem.* **2008**, *18*, 5468–5474. [[CrossRef](#)]
28. Zhang, F.; Jespersen, K.G.; Bjoerstroem, C.; Svensson, M.; Andersson, M.R.; Sundström, V.; Magnusson, K.; Moons, E.; Yartsev, A.; Inganäs, O. Influence of solvent mixing on the morphology and performance of solar cells based on polyfluorene copolymer/fullerene blends. *Adv. Funct. Mater.* **2006**, *16*, 667–674. [[CrossRef](#)]
29. Alghamdi, A.A.; Watters, D.C.; Yi, H.; Al-Faifi, S.; Almeataq, M.S.; Coles, D.; Kingsley, J.; Lidzey, D.G.; Iraqi, A. Selenophene vs. thiophene in benzothiadiazole-based low energy gap donor–acceptor polymers for photovoltaic applications. *J. Mater. Chem. A* **2013**, *1*, 5165–5171. [[CrossRef](#)]
30. Watters, D.C.; Yi, H.; Pearson, A.J.; Kingsley, J.; Iraqi, A.; Lidzey, D. Fluorene-Based Co-polymer with High Hole Mobility and Device Performance in Bulk Heterojunction Organic Solar Cells. *Macromol. Rapid Commun.* **2013**, *34*, 1157–1162. [[CrossRef](#)]
31. Pearson, A.J.; Watters, D.C.; Yi, H.; Sarjadi, M.S.; Reynolds, L.X.; Marchisio, P.P.; Kingsley, J.; Haque, S.A.; Iraqi, A.; Lidzey, D.G. Impact of dithienyl or thienothiophene units on the optoelectronic and photovoltaic properties of benzo [1, 2, 5] thiadiazole based donor–acceptor copolymers for organic solar cell devices. *RSC Adv.* **2014**, *4*, 43142–43149. [[CrossRef](#)]
32. Chen, C.-H.; Hsieh, C.-H.; Dubosc, M.; Cheng, Y.-J.; Hsu, C.-S. Synthesis and characterization of bridged bithiophene-based conjugated polymers for photovoltaic applications: Acceptor strength and ternary blends. *Macromolecules* **2009**, *43*, 697–708. [[CrossRef](#)]
33. Kitazawa, D.; Watanabe, N.; Yamamoto, S.; Tsukamoto, J. Quinoxaline-based pi-conjugated donor polymer for highly efficient organic thin-film solar cells. *Appl. Phys. Lett.* **2009**, *95*, 3701.
34. Boudreault, P.L.T.; Michaud, A.; Leclerc, M. A New Poly (2, 7-Dibenzosilole) Derivative in Polymer Solar Cells. *Macromol. Rapid Commun.* **2007**, *28*, 2176–2179. [[CrossRef](#)]
35. Wang, E.; Wang, L.; Lan, L.; Luo, C.; Zhuang, W.; Peng, J.; Cao, Y. High-performance polymer heterojunction solar cells of a polysilafluorene derivative. *Appl. Phys. Lett.* **2008**, *92*, 33307. [[CrossRef](#)]
36. Chen, H.Y.; Hou, J.; Hayden, A.E.; Yang, H.; Houk, K.; Yang, Y. Silicon Atom Substitution Enhances Interchain Packing in a Thiophene-Based Polymer System. *Adv. Mater.* **2010**, *22*, 371–375. [[CrossRef](#)]
37. Ponomarenko, S.; Muzafarov, A.; Borshchev, O.; Vodopyanov, E.; Demchenko, N.; Myakushev, V. Synthesis of bithiophenesilane dendrimer of the first generation. *Russ. Chem. Bull.* **2005**, *54*, 684–690. [[CrossRef](#)]
38. Wen, L.; Rasmussen, S.C. Synthesis and structural characterization of 2, 5-dihalo-3, 4-dinitrothiophenes. *J. Chem. Crystallogr.* **2007**, *37*, 387–398. [[CrossRef](#)]
39. Schwiderski, R.L.; Rasmussen, S.C. Synthesis and Characterization of Thieno [3, 4-b] pyrazine-Based Terthienyls: Tunable Precursors for Low Band Gap Conjugated Materials. *J. Org. Chem.* **2013**, *78*, 5453–5462. [[CrossRef](#)]

40. Hailu, H.; Atsbeha, B.; Admassie, S.; Mammo, W.; Raju, V.; Chebude, Y. Variable denticity of a multidentate terthiophene derivative towards Ni (II) and Zn (II)—structural studies. *Bull. Chem. Soc. Ethiop.* **2011**, *25*, 221–231. [[CrossRef](#)]
41. Delgado, M.R.; Hernandez, V.; Navarrete, J.L.; Tanaka, S.; Yamashita, Y. Combined spectroscopic and theoretical study of narrow band gap heterocyclic co-oligomers containing alternating aromatic donor and o-quinoid acceptor units. *J. Phys. Chem. B* **2004**, *108*, 2516–2526. [[CrossRef](#)]
42. Lan, L.; Chen, Z.; Li, Y.; Ying, L.; Huang, F.; Cao, Y. Donor–acceptor conjugated polymers based on cyclic imide substituted quinoxaline or dibenzo [a, c] phenazine for polymer solar cells. *Polym. Chem.* **2015**, *6*, 7558–7569. [[CrossRef](#)]
43. Matsueda, Y.; Xu, S.; Negishi, E.-I. A novel highly enantio- and diastereoselective synthesis of vitamin E side-chain. *Tetrahedron Lett.* **2015**, *56*, 3346–3348. [[CrossRef](#)]
44. Thomson, A.; O'Connor, S.; Knuckley, B.; Causey, C.P. Synthesis, and in vitro evaluation of an activity-based protein profiling (ABPP) probe targeting agmatine deiminases. *Bioorg. Med. Chem.* **2014**, *22*, 4602–4608. [[CrossRef](#)]
45. Yue, W.; Zhao, Y.; Shao, S.; Tian, H.; Xie, Z.; Geng, Y.; Wang, F. Novel NIR-absorbing conjugated polymers for efficient polymer solar cells: Effect of alkyl chain length on device performance. *J. Mater. Chem.* **2009**, *19*, 2199–2206. [[CrossRef](#)]
46. Lu, G.; Usta, H.; Risko, C.; Wang, L.; Facchetti, A.; Ratner, M.A.; Marks, T.J. Synthesis, characterization, and transistor response of semiconducting silole polymers with substantial hole mobility and air stability. Experiment and theory. *J. Am. Chem. Soc.* **2008**, *130*, 7670–7685. [[CrossRef](#)]
47. Yang, J.; Sun, N.; Huang, J.; Li, Q.; Peng, Q.; Tang, X.; Dong, Y.; Ma, D.; Li, Z. New AIEgens containing tetraphenylethene and silole moieties: Tunable intramolecular conjugation, aggregation-induced emission characteristics and good device performance. *J. Mater. Chem. C* **2015**, *3*, 2624–2631. [[CrossRef](#)]
48. Keyworth, C.W.; Chan, K.L.; Labram, J.G.; Anthopoulos, T.D.; Watkins, S.E.; McKiernan, M.; White, A.J.; Holmes, A.B.; Williams, C.K. The tuning of the energy levels of dibenzosilole copolymers and applications in organic electronics. *J. Mater. Chem.* **2011**, *21*, 11800–11814. [[CrossRef](#)]
49. Usta, H.; Lu, G.; Facchetti, A.; Marks, T.J. Dithienosilole- and dibenzosilole-thiophene copolymers as semiconductors for organic thin-film transistors. *J. Am. Chem. Soc.* **2006**, *128*, 9034–9035. [[CrossRef](#)]
50. Chan, K.L.; McKiernan, M.J.; Towns, C.R.; Holmes, A.B. Poly (2, 7-dibenzosilole): A blue light emitting polymer. *J. Am. Chem. Soc.* **2005**, *127*, 7662–7663. [[CrossRef](#)]
51. Kenning, D.D.; Mitchell, K.A.; Calhoun, T.R.; Funfar, M.R.; Sattler, D.J.; Rasmussen, S.C. Thieno[3,4-b]pyrazines: Synthesis, structure, and reactivity. *J. Org. Chem.* **2002**, *67*, 9073–9076. [[CrossRef](#)]
52. McNamara, L.E.; Liyanage, N.; Peddapuram, A.; Murphy, J.S.; Delcamp, J.H.; Hammer, N.I. Donor-Acceptor-Donor Thienopyrazines via Pd-Catalyzed C-H Activation as NIR Fluorescent Materials. *J. Org. Chem.* **2015**, *81*, 32–42. [[CrossRef](#)] [[PubMed](#)]
53. Heinze, J.; Frontana-Urbe, B.A.; Ludwigs, S. Electrochemistry of conducting polymers-persistent models and new concepts. *Chem. Rev.* **2010**, *110*, 4724–4771. [[CrossRef](#)] [[PubMed](#)]
54. Hadi, J.M.; Aziz, S.B.; Nofal, M.M.; Hussien, S.A.; Hamsan, M.H.; Brza, M.A.; Abdulwahid, R.T.; Kadir, M.F.Z.; Woo, H.J. Electrical, dielectric property and electrochemical performances of plasticized silver ion-conducting chitosan-based polymer nanocomposites. *Membranes* **2020**, *10*, 151. [[CrossRef](#)] [[PubMed](#)]
55. Aziz, S.B.; Hamsan, M.H.; Nofal, M.M.; San, S.; Abdulwahid, R.T.; Saeed, S.R.R.; Brza, M.A.; Kadir, M.F.Z.; Mohammed, S.J.; Al-Zangana, S. From Cellulose, Shrimp and Crab Shells to Energy Storage EDLC Cells: The Study of Structural and Electrochemical Properties of Proton Conducting Chitosan-Based Biopolymer Blend Electrolytes. *Polymers* **2020**, *12*, 1526. [[CrossRef](#)] [[PubMed](#)]
56. Brza, M.A.; Aziz, S.B.; Anuar, H.; Ali, F.; Hamsan, M.H.; Kadir, M.F.Z.; Abdulwahid, R.T. Metal framework as a novel approach for the fabrication of electric double layer capacitor device with high energy density using plasticized Poly(vinyl alcohol): Ammonium thiocyanate based polymer electrolyte. *Arab. J. Chem.* **2020**, *13*, 7247–7263. [[CrossRef](#)]
57. Aziz, S.B.; Abdulwahid, R.T.; Rsaul, H.A.; Ahmed, H.M. In situ synthesis of CuS nanoparticle with a distinguishable SPR peak in NIR region. *J. Mater. Sci. Mater. Electron.* **2016**, *27*, 4163–4171. [[CrossRef](#)]
58. Abdulwahid, R.T.; Abdullah, O.G.; Aziz, S.B.; Hussein, S.A.; Muhammad, F.F.; Yahya, M.Y. The study of structural and optical properties of PVA:PbO₂ based solid polymer nanocomposites. *J. Mater. Sci. Mater. Electron.* **2016**, *27*, 12112–12118. [[CrossRef](#)]

59. Asnawi, A.S.F.M.; Aziz, S.B.; Nofal, M.M.; Hamsan, M.H.; Brza, M.A.; Yusof, Y.M.; Abdulwahid, R.T.; Muzakir, S.K.; Kadir, M.F.Z. Glycerolized Li⁺ ion conducting chitosan-based polymer electrolyte for energy storage EDLC device applications with relatively high energy density. *Polymers* **2020**, *12*, 1433. [[CrossRef](#)]
60. Echeverri, M.; Hamad, C.; Kyu, T. Highly conductive, completely amorphous polymer electrolyte membranes fabricated through photo-polymerization of poly (ethylene glycol diacrylate) in mixtures of solid plasticizer and lithium salt. *Solid State Ion.* **2014**, *254*, 92–100. [[CrossRef](#)]
61. Li, L.; Wang, X.; Zhu, P.; Li, H.; Wang, F.; Wu, J. The electron transfer mechanism between metal and amorphous polymers in humidity environment for triboelectric nanogenerator. *Nano Energy* **2020**, *70*, 104476. [[CrossRef](#)]

Publisher's Note: MDPI stays neutral with regard to jurisdictional claims in published maps and institutional affiliations.



© 2020 by the authors. Licensee MDPI, Basel, Switzerland. This article is an open access article distributed under the terms and conditions of the Creative Commons Attribution (CC BY) license (<http://creativecommons.org/licenses/by/4.0/>).